



A persistent feature of multiple scattering of waves in the time-domain: A tutorial

James A. Lock^{a,*}, Michael I. Mishchenko^b

^a Physics Department, Cleveland State University, Cleveland, OH 44115, USA

^b NASA Goddard Institute for Space Studies, 2880 Broadway, New York, NY 10025, USA



ARTICLE INFO

Article history:

Received 10 December 2014

Received in revised form

25 February 2015

Accepted 26 February 2015

Available online 6 March 2015

Keywords:

Wave scattering
Multiple scattering
Frequency-domain
Time-domain
Particles

ABSTRACT

The equations for frequency-domain multiple scattering are derived for a scalar or electromagnetic plane wave incident on a collection of particles at known positions, and in the time-domain for a plane wave pulse incident on the same collection of particles. The calculation is carried out for five different combinations of wave types and particle types of increasing geometrical complexity. The results are used to illustrate and discuss a number of physical and mathematical characteristics of multiple scattering in the frequency- and time-domains. We argue that frequency-domain multiple scattering is a purely mathematical construct since there is no temporal sequencing information in the frequency-domain equations and since the multi-particle path information can be dispelled by writing the equations in another mathematical form. However, multiple scattering becomes a definite physical phenomenon in the time-domain when the collection of particles is illuminated by an appropriately short localized pulse.

© 2015 Elsevier Ltd. All rights reserved.

1. Introduction

The subject of this tutorial is the physical and mathematical interpretation of the equations of multiple scattering of waves in the frequency- and time-domains. Martin (see Sec. 1.1 of [1]) has correctly remarked that “multiple scattering” may mean different things to different scientists. We should add that the meaning of the term “multiple scattering” can also vary depending on the particular context in which it appears. More often than not, this has to do with the fact that although physics describes actual natural phenomena, it does so using the abstract language of mathematics. It is therefore important to delineate the situations when multiple scattering represents a real physical process and those when it emerges as a purely mathematical construct.

In the frequency-domain, a monochromatic plane wave or shaped beam of infinite temporal duration is incident

on a collection of scattering particles at known fixed positions. Five attributes of multiple scattering of waves in the *frequency-domain* have recently been described in [2–5] and pp. 6–9, 47, 65–66 of [6] in order to clarify a number of common misconceptions. They are as follows.

- (i) If one wishes to discuss wave scattering by a collection of many particles in terms of multiple scattering, the so-called compact form of the pertinent equations can be expanded, purely mathematically, as a particular infinite series of terms known as the expanded form of the equations [7]. This series has been called the multiple-scattering point of view [8], an order-of-scattering expansion [9–11], or a multi-path expansion of the total wave (see [7] and pp. 765–766 of [12]).
- (ii) The multiple-scattering point of view in the frequency-domain with the incident wave being scattered sequentially by one, two, three, or more particles before reaching the observation point does not refer to an actual physical phenomenon. It is only a purely mathematical expansion of the total wave. This is because in the frequency-domain

* Corresponding author.

E-mail address: j.lock@csuohio.edu (J.A. Lock).

- all the mutual excitations occur simultaneously and are not temporally discrete and ordered events.
- (iii) The scattered wave leaving particle i to be rescattered by particle j does not propagate only in the specific direction from i to j as is the case for a multiply-scattered projectile particle.
 - (iv) For frequency-domain scattering in general, the scattering equations are consistent with the point of view that the wave incident on particle j is not transformed into or replaced by the scattered wave. Thus the cause of scattering at particle j is not the incident field, but rather the presence of an object with physical properties different from that of the external medium.
 - (v) The form of the total field in the exterior medium makes it clear that both the incident and scattered fields, considered individually, are purely mathematical entities rather than actual physical objects. The only actual physical object is the total field, either in the presence of or in the absence of the scattering particle. The scattered field is defined to be the difference between the total field in the exterior region with and without the scatterer present.

To demonstrate that the situation can be profoundly different in the time-domain, in the body of this tutorial we describe exactly soluble time-domain multiple scattering scenarios involving an incident narrow Gaussian plane wave pulse. We obtain the solutions for five fixed (deterministic) scattering objects of increasing geometric complexity and analyze them using four different mathematical approaches.¹ The examples considered here are used to revisit, and refine where necessary, the above *frequency-domain* statements (i)–(v) formulated for an incident beam of infinite temporal duration. They are also used to extend some of the statements when one considers *time-domain* scattering of a temporally-short incident pulse. The specific selection of the five scattering scenarios of increasing complexity is intended to maximize the pedagogical value of our discussion for the reader.

We start with the simple examples of one-dimensional scattering, and then isotropic scattering of scalar waves in three dimensions. Then we progress to the more complicated and realistic situations of particles of finite size, arbitrary shape and internal composition, and incident electromagnetic waves rather than scalar waves. As the examples become more elaborate and complicated, the mathematics and notation needed to fully and accurately describe them become more elaborate and complicated as well. This is why we consider the simplest geometries first, in order to avoid the complexity of the notation from obscuring the patterns that occur in the equations and the points we are trying to illustrate.

In spite of the increased complexity as we progress from example to example, certain time-domain multiple-scattering phenomena occur in exactly the same way time

after time, i.e. they persist. Specifically, scattering of a temporally-short pulse results in a temporal succession of distinct individual scattered pulses in a one-to-one correspondence with the different multi-particle paths encountered in the frequency-domain. This result is obtained by first separating out all the rapidly-varying wave number-dependent phases in the terms of the expanded form of the frequency-domain multiple scattering equations. The mathematical details of this separation turn out to be different for the different examples considered. The resulting temporal succession of pulses obtained in the time-domain is not valid for only the simplest of examples, but persists as the geometrical complexity of the system increases. As a result, the pulse sequence has the effect of elevating multiple scattering from being an abstract mathematical entity in the *frequency-domain* to an actual physical phenomenon in the *time-domain*.

2. General considerations

Before describing the five multiple scattering scenarios in detail, it is instructive to discuss the definition of a number of terms used throughout this tutorial. The first of these, as in statement (v) of Section 1, is the difference between purely mathematical entities and actual physical objects. In Lorenz–Mie scattering a linearly polarized monochromatic electromagnetic plane wave having infinite transverse extent and infinite temporal duration, angular frequency ω , wavelength λ , and wave-number $k=2\pi/\lambda$ is incident on a single spherical particle of radius a and refractive index N whose center is at the origin of coordinates. The scalar radiation potential (see Sec. 9.21 of [13]) of the total wave exterior to the particle satisfies the scalar wave equation subject to the appropriate boundary conditions, and is standardly chosen to have the form

$$\psi_{total}(\mathbf{kr})\exp(-i\omega t) = \psi_{beam}(\mathbf{kr})\exp(-i\omega t) + \psi_{scatt}(\mathbf{kr})\exp(-i\omega t), \quad (1)$$

where the electromagnetic fields of the incident and scattered waves are obtained by vector differentiation of ψ_{beam} and ψ_{scatt} , respectively. In Eq. (1), \mathbf{r} is the position vector, t is time, and $i=(-1)^{1/2}$. The motivation of the assumption that the incident wave is present in the entirety of the exterior region is due to the fact that the portion of it that is transversely distant from the scattering particle passes from upstream locations to downstream locations without ever directly encountering the particle or being diffracted by it. It was stated in [2–6] that the only wave with a definite physical existence in this situation is ψ_{total} , and the decomposition of ψ_{total} into the sum of ψ_{beam} and ψ_{scatt} is a purely mathematical construction.

This is an instance of a more fundamental problem: if a wave ψ_{total} is decomposed into the sum of two hypothetical parts ψ_1 and ψ_2 ,

$$\psi_{total} = \psi_1 + \psi_2, \quad (2)$$

when is such a decomposition purely an abstract mathematical construction and when do the two parts have a definite physical existence? The answer depends crucially on the details of the experimental configuration and the attributes of the two hypothetical parts. If an experiment

¹ We note that stochastic scattering objects in the form of a group of particles located at statistically random positions involve a number of issues that will not be discussed here. Moving scatterers will also not be considered, since their analysis lies in the realm of dynamic light scattering.

can be performed that filters out one of the parts and simultaneously measures the other at a single instant of time, and obtains the expected answer for the properties of the remaining part in the absence of the filtered part, then one may justifiably claim that each of the parts has an independent physical existence. If such an experiment cannot be performed, or if the results do not correspond to the presumed properties of the hypothetical parts, then one can claim that the decomposition is purely a mathematical construction.

We illustrate this point of view with the following simple example. Consider a beam exiting a laser and expanded by a pair of lenses. We assume that the expanded laser beam in the spatial region of interest can be modeled by a plane wave whose electric field is

$$\mathbf{E}_{total}(\mathbf{r}, t) = E_0 \mathbf{u}_x \exp(ikz - i\omega t), \quad (3)$$

where \mathbf{u}_x is a unit vector in the positive x direction. One can mathematically write this field as

$$\mathbf{E}_{total}(\mathbf{r}, t) = E_1 \mathbf{u}_x \exp(ikz - i\omega t) + E_2 \mathbf{u}_x \exp(ikz - i\omega t), \quad (4)$$

where

$$E_1 = E_0/2, \quad (5a)$$

$$E_2 = E_0/2. \quad (5b)$$

Both hypothetical component beams have exactly the same frequency, phase, direction of travel, and polarization. There is no difference in any of these attributes that can be used to filter one of the components out while retaining the other. So one would say that the decomposition of Eqs. (4) and (5) is purely mathematical for this geometry.

Now consider the same total beam with the same decomposition, but occurring in the context of a different geometry. An original expanded laser beam is passed through an interferometer with equal length arms. The E_1 beam has traversed arm 1 of the interferometer, and the E_2 beam has traversed arm 2. The total recombined beam in the spatial region of interest is $\mathbf{E}_{total}(\mathbf{r}, t)$ of Eq. (3). There is now a difference between the two identical-looking components in this new experiment. Although they continue to have the same frequency, phase, direction of travel, and polarization, they have different histories. Blocking arm 1 results in detecting only the second component, while blocking arm 2 results in detecting only the first component. The results of the arm-blocking experiments will always record the time-average intensity $(1/4)(E_0^2/2\mu_0 c)$, where μ_0 is the permeability of free space and c is the corresponding speed of light, agreeing with the postulated decomposition of Eqs. (5a) and (5b). Due to the details of this new geometrical configuration, the two component beams in the spatial region of interest now have an independent physical reality. However, the postulated decomposition of Eq. (4) for the interferometer geometry with

$$E_1 = 3E_0/4, \quad (6a)$$

$$E_2 = E_0/4 \quad (6b)$$

is purely a mathematical decomposition because arm-blocking experiments will never record the component energies $(9/16)(E_0^2/2\mu_0 c)$ or $(1/16)(E_0^2/2\mu_0 c)$.

However, the arm-blocking experiments described here, and filtering experiments in general, are in some sense incomplete. A particular boundary value problem for the wave equation has been posed, and in the spatial region of interest, its solution is ψ_{total} . Even if it is physically comprised of a number of components, the fact that ψ_{total} is the actual solution to the specific frequency-domain boundary value problem that was posed gives it a degree of primacy over the individual components. This is because if the energy of each of the individual components, $\psi_1^* \psi_1$ or $\psi_2^* \psi_2$ where the asterisk denotes complex conjugation, is separately recorded in filtering experiments, the sum of these energies will not be equal to the energy contained in ψ_{total} ,

$$\psi_1^* \psi_1 + \psi_2^* \psi_2 \neq \psi_{total}^* \psi_{total}. \quad (7)$$

Since the filtering experiments described here delete either ψ_1 or ψ_2 , they cannot record the energy content of the interference of the two component waves $\psi_1^* \psi_2 + \psi_2^* \psi_1$, which is an integral contribution to the energy content of ψ_{total} .

The way in which this point of view applies to Lorenz–Mie scattering is that the electromagnetic waves derived from ψ_{beam} and ψ_{scatt} of Eq. (1) almost always have different directions of travel or different polarizations. The differences in these features imply the possibility that an experiment can be performed that filters out one or the other component wave and measures some of the features of the remaining component. For example, a far-zone detector in a Lorenz–Mie scattering experiment is placed at the polar angle $\theta_{p0} = 150^\circ$. Since the sensitive face of the detector (e.g. the eye of the observer) points toward the scattering particle and away from the propagation of the incident beam (e.g. the incoming plane wave strikes the back of the observer's head), only the scattered wave will be detected. If the detector were instead rotated in place so that its sensitive face now faces the incoming beam and the scattered wave strikes the back side of the detector, only the incident beam will be detected. Similarly, if a polarizing filter is placed in front of a suitably positioned detector so as to filter out the linearly polarized incident beam, the recorded signal is due to the portion of the scattered wave having the orthogonal polarization. The recorded energy of the scattered wave for this filtering experiment has been shown to agree with the predictions of Lorenz–Mie theory. This separation of the incident and scattered waves, however, is not always possible. As was pointed out in [14], if a plane wave is incident on a totally opaque sphere, the incident and scattered waves at off-axis positions immediately behind the particle have the same direction of travel and polarization, but are 180° out of phase with each other. Their destructive interference causes the so-called deep shadow region immediately behind the particle (see Fig. 2 of [14] and Fig. 14 of [15]). The components of the total wave are not physically separable in this shadow region.

As a refinement to statement (v) of Section 1, one can infer that for the decomposition of the total wave in the exterior region into the incident beam and scattered wave as in Eq. (1), each of these components can be said to have an independent physical existence almost everywhere exterior to the particle. If the total wave were decomposed

into the sum of two or more components in any one of a number of differing ways that are not realized in various filtering experiments, the decomposition would remain purely mathematical in nature. An additional corollary to statement (v) is that the total wave enjoys a degree of primacy over the two component waves since it is the solution of the posed electromagnetic boundary value problem, and as such, filtering experiments cannot access the cross-term energy components of the total wave.

We next revisit statement (ii) of Section 1 as to whether multiple scattering in the frequency-domain is an actual physical process, or whether it is a purely mathematical entity. Approaching this from a historical perspective, the study of multiple scattering of waves began in earnest in the second half of the 1940s and the early 1950s [7–10,16,17]. The original compact form of the integral equations describing scattering of the incident beam in the frequency-domain was iterated to obtain an infinite series, or extended form of the equations, assuming the interaction of the incident wave with the particles was weak enough so that the iteration series converged. The terms of the extended form contained differing numbers of ordered single-scattering events, which we will call multi-particle paths. From a mathematical point of view, we claim that multiple scattering in the frequency-domain is a mathematical construct and does not correspond to a real physical phenomenon. This is because the multiple-scattering interpretation suggested by the expanded form of the equations can be transformed away or hidden by using a different but mathematically equivalent form of the equations, i.e. the compact form. For it to be a real phenomenon the signature of multiple scattering as a temporally ordered sequence of individual single-scattering events must be fully and equally present no matter which mathematically equivalent method is used to write the equations. The same conclusion can be arrived at from a more physical argument. Since an incident beam in the frequency-domain has infinite temporal duration, it is always traveling past and washing over the scattering particles, creating scattered waves. As a result, all of the scatterings and rescatterings that can occur, are always occurring, and are always spatially interfering with each other. Thus, we claim that frequency-domain multiple scattering is not a real physical process because it does not include the temporal sequencing necessary to fully characterize multiple scattering. That is the prerogative of time-domain scattering.

Although the multi-particle path interpretation of frequency-domain multiple scattering is a purely mathematical construct, it is a very suggestive and fruitful one. In the context of the example described in Section 4, it forms the basis of diffusing wave spectroscopy for the dynamic light scattering characterization of concentrated colloidal suspensions in the deep multiple scattering limit [18,19] and the interaction of sound waves with the bubble cloud present in the wake of a submarine [16]. In the context of the example of Section 7 it is also used to derive the equation of radiative transfer for a sparse collection of scatterers as an approximation, beginning from exact electromagnetic equations (see Sec. 14.7 of [20], and [21]). It also sets the stage for multiple scattering in the time-domain (see [22] and Sec. 11.2 of [23]),

where subject to certain geometrical conditions, when one explicitly keeps track of the rapidly-varying portion of the phase of the scattered light, scattering of a temporally-short pulse results in a temporal succession of scattered pulses that are in a one-to-one correspondence with the different multi-particle paths in the frequency-domain. This temporal sequence of scattered pulses cannot be hidden or transformed away by writing the solution to the multiple scattering equations in a different form or by solving the original time-dependent differential equation using a different method. Our extension to statement (ii) of Section 1 is that this persistent feature of time-domain multiple scattering raises it above being purely a mathematical abstraction obtained by writing the solution to the problem in a particular form. It becomes a real physical process unfolding in time.

3. Transmission and reflection of a normally incident wave by a slab having two parallel interfaces

The frequency-domain multiple scattering equations of the five examples described in Sections 3–7 are all well-known. Our emphasis in obtaining these equations will be on explicitly factoring out the rapidly-varying portion of the phase of each of the multi-particle paths of the expanded form so as to smoothly lead into the time-domain version of the example. Consider first the one-dimensional example where a coherent monochromatic plane wave $\psi(z, t)$ with wavelength λ , wave-number $k_1 = 2\pi/\lambda$, and angular frequency ω , is propagating in the $+z$ direction for $z < 0$. It is incident on an infinitely wide slab of homogeneous material with the known endpoints $z=0$ and $z=L$, parameterized by a well potential $V(z)$ of constant strength $-V_0$ with $V_0 > 0$. The external medium for $z < 0$ is denoted as medium 1, the well region as region 2, and the external medium for $z > L$ as region 3. The 12 interface separates regions 1 and 2 and the 23 interface separates regions 2 and 3. A percentage of the incident wave is reflected by the well back into region 1, and part is transmitted through it into region 3. The wave-number of the wave in the well region is taken to be k_2 , and it is again k_1 in region 3. This geometry describes a number of different types of waves, including a normally incident linearly polarized electromagnetic wave whose electric and magnetic field vectors point in the $+x$ and $+y$ directions, respectively. We analyze this simple one-dimensional example in detail because it illustrates many important features of multiple scattering in both the frequency- and time-domains, as was noted in [24,25].

The time evolution of an electromagnetic wave for this geometry satisfies the one-dimensional classical wave equation

$$\frac{\partial^2 \psi}{\partial z^2} = \frac{N^2(z)}{c^2} \frac{\partial^2 \psi}{\partial t^2}, \quad (8)$$

where $\psi(z, t)$ is the electric field strength, $N(z)$ is the refractive index of the medium, and c is the speed of light in the exterior medium. The constant refractive index of region 2 relative to that of the external medium is N_2 , and the resulting effective well strength in region 2 is (see Eq. (1.9)

of [26])

$$-V_0 = -k_1^2(N_2^2 - 1). \tag{9}$$

Substituting a plane wave for $\psi(z, t)$ into Eq. (8), the dispersion relation for the waves is

$$\omega = ck_1 = ck_2/N_2. \tag{10}$$

The relation between k_1 and k_2 in Eq. (10) is only slightly nonlinear since N_2 for dielectric materials such as water [27] or glass (see p. 463, Table 23I of [28]) only weakly depends on k_1 in the visible and near infra-red regions. This slight nonlinearity will hereafter be ignored. The wave amplitude in region j will be denoted by $\psi_j(z, t)$ for $j=1, 2, 3$. Since the wave is assumed to be monochromatic,

$$\psi_j(z, t) = \psi_j(z)\exp(-i\omega t), \tag{11}$$

and the time-independent wave equation arising from Eq. (8) becomes

$$\frac{d^2\psi_j}{dz^2} + k_j^2\psi_j(z) = 0, \tag{12}$$

subject to the boundary conditions that the tangential components of the electric and magnetic fields are continuous at the 12 and 23 interfaces, which is equivalent to the continuity of ψ and $d\psi/dz$.

We assume that a monochromatic plane wave with amplitude A is incident on the 12 interface from the left in region 1. The standard solution to this problem, with the $\exp(-i\omega t)$ dependence of each term temporarily left implicit, is

$$\psi_1(k_1, z) = A \exp(ik_1z) + B \exp(-ik_1z), \tag{13a}$$

$$\psi_2(k_1, z) = C \cos(k_2z) + D \sin(k_2z), \tag{13b}$$

$$\psi_3(k_1, z) = E \exp(ik_1z). \tag{13c}$$

The second term in Eq. (13a) is interpreted as the reflected wave, the two terms in Eq. (13b) are Fabry–Perot standing waves in the well region, and Eq. (13c) is the transmitted wave. If instead one wanted to emphasize the presence of traveling waves in region 2, one could write

$$\psi_2(k_1, z) = C' \exp(ik_2z) + D' \exp(-ik_2z), \tag{14a}$$

where

$$C = (C' + D')/2, \tag{14b}$$

$$D = (C' - D')/(2i). \tag{14c}$$

It should be noted that since the implicit time dependence in each term of Eqs. (13a)–(13c) and (14a) is assumed to be $\exp(-i\omega t)$, all the time-dependent effects of retardation (see Sec. 10.2.1 of [29]) are contained in the as-of-yet unknown coefficients B, C, D , and E . It should also be noted that the standard form of the solution in Eqs. (13a) and (13c) differs from that of Eq. (1) in Lorenz–Mie theory. This is motivated by the fact that since both the incident plane wave and the well region in this example are of infinite transverse extent, the only way a portion of the incident wave can get from $z < 0$ upstream with respect to the well to $z > L$ downstream is by going through it.

By applying the four boundary conditions at $z=0$ and $z=L$, the four unknown coefficients B, C, D , and E can be evaluated to give

$$B = iA(k_2^2 - k_1^2) \sin(k_2L)/G, \tag{15a}$$

$$C = 2Ak_1k_2 \exp(ik_2L)/G, \tag{15b}$$

$$D = 2iAk_1^2 \exp(ik_2L)/G, \tag{15c}$$

$$E = 2Ak_1k_2 \exp(-ik_1L)/G, \tag{15d}$$

where

$$G = 2k_1k_2 \cos(k_2L) - i(k_1^2 + k_2^2) \sin(k_2L). \tag{15e}$$

The problem has now been solved. This form of the solution, i.e. the compact form, is the most practical form the solution can take if one is interested in numerically calculating the percentage of the incoming wave intensity that is either transmitted or reflected,

$$T = E^*E/(A^*A), \tag{16a}$$

$$R = B^*B/(A^*A). \tag{16b}$$

Although Eqs. (15a)–(15e) provide a convenient and useful solution to the original differential equation (12) subject to the boundary conditions at $z=0$ and $z=L$, they give no clue as to the physical mechanism or mechanisms responsible for producing the observed transmitted or reflected wave intensity. In particular, the transmitted intensity is found to have an enhancement or resonance when $2N_2L$ is equal to an integer number of wavelengths, while the reflected intensity has a resonance when $2N_2L$ is equal to a half-integer number of wavelengths (see Sec. 6.8 of [23]). These resonances result from the action of a significant physical mechanism. In order to suggest, though not yet prove, such a mechanism, Eqs. (15a)–(15e) can be rewritten in an expanded form that is not especially well-suited for numerical evaluation of Eqs. (16a) and (16b). Defining

$$t_{12} = 2k_1/(k_2 + k_1), \tag{17a}$$

$$t_{21} = 2k_2/(k_2 + k_1), \tag{17b}$$

$$r_{121} = -(k_2 - k_1)/(k_2 + k_1), \tag{17c}$$

$$r_{212} = (k_2 - k_1)/(k_2 + k_1), \tag{17d}$$

it can be shown that since $|r_{212}| < 1$, Eqs. (13a)–(13c) with the coefficients of Eqs. (15a)–(15d) may be written as a converging geometric series,

$$\begin{aligned} \psi_1(k_1, z) = & A \exp(ik_1z) + A \exp(-ik_1z) \\ & \times \left\{ r_{121} + t_{21} \left[\sum_{n=0}^{\infty} [(\exp(ik_2L)r_{212} \exp(ik_2L)r_{212})^n] \right] \right. \\ & \left. \times \exp(ik_2L)r_{212} \exp(ik_2L)t_{12} \right\}, \end{aligned} \tag{18a}$$

$$\begin{aligned} \psi_2(k_1, z) = & A \exp(ik_2z) \left\{ \sum_{n=0}^{\infty} [r_{212} \exp(ik_2L)r_{212} \exp(ik_2L)]^n \right\} t_{12} \\ & + A \exp[-ik_2(z-L)] \end{aligned}$$

$$\begin{aligned} & \times \left\{ \sum_{n=0}^{\infty} [r_{212} \exp(ik_2L)r_{212} \exp(ik_2L)]^n \right\} r_{212} \\ & \times \exp(ik_2L)t_{12}, \end{aligned} \quad (18b)$$

$$\begin{aligned} \psi_3(k_1, z) &= A \exp[ik_1(z-L)] t_{21} \\ & \times \left\{ \sum_{n=0}^{\infty} [\exp(ik_2L)r_{212} \exp(ik_2L)r_{212}]^n \right\} \exp(ik_2L)t_{12}. \end{aligned} \quad (18c)$$

This representation of the coefficients B , C , D , and E as an infinite series is not unique. The coefficients could have been rewritten in a very large number of different, but mathematically equivalent, ways. What makes the particular series representation of Eqs. (18a)–(18c) special is that it suggests, though does not yet prove, the physical mechanism responsible for understanding the observed amount of transmission and reflection of Eqs. (16a) and (16b). The mechanism is suggested in Fig. 1. If a wave in region 1 were incident from the left on a single 12 interface, the Fresnel coefficient for the transmitted wave amplitude into region 2 is t_{12} as given by Eq. (17a), and the wave amplitude reflected back into region 1 is r_{121} as given by Eq. (17c). Similarly, if a wave in region 2 were incident on a single 23 interface from the right or a single 21 interface from the left, the Fresnel coefficient for the transmitted wave amplitude into region 1 or region 3 is t_{21} as given by Eq. (17b), and the wave amplitude reflected back into region 2 is r_{212} as given by Eq. (17d). The suggested, though not yet proven, multiple-scattering interpretation of Eq. (18c) for transmission is that, reading the factors in Eq. (18c) from right to left, the incident wave is first partially transmitted from region 1 into region 2. It then traverses the well region acquiring the phase $\exp(ik_2L)$. It then partially reflects back and forth n times inside region 2 losing amplitude but acquiring more phase each time, and is finally partially transmitted from region 2 into region 3. Once in region 3 the transmitted wave travels the additional distance $z-L$, acquiring the phase $\exp[ik_1(z-L)]$ before arriving at the location z . The k -dependent phase of each multiple-scattering transmission path is equal to the optical path length that a geometrical light ray would have traversed, reflecting back and forth n times between the interfaces before exiting in the forward direction. The amplitudes of the individual

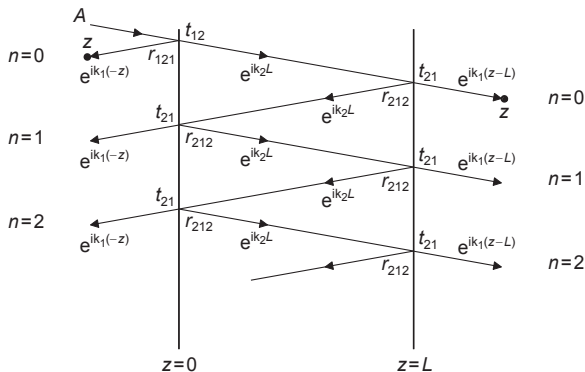


Fig. 1. Multiple-scattering paths associated with the reflected, interior, and transmitted waves of Eqs. (18a)–(18c), showing the phase advance, and transmission and reflection amplitude of each equivalent ray path.

transmission paths are then superposed and interfere to produce the total transmitted amplitude at z . The multi-path interpretation for the reflected wave of Eq. (18a) and the waves in the well region of Eq. (18b) is similar, again reading the factors from right to left. The k -dependent phase of each reflected path is again equal to the optical path length a ray would have traversed before exiting the interfaces in the backward direction. The amplitudes of the individual reflection paths are again superposed and interfere to produce the total reflected amplitude at z . The multi-interaction path interpretation of the solution is encoded in the k -dependent phase of each term. The transmission resonances mentioned above are then interpreted as being due to constructive interference of the successive transmitted rays, and the reflection resonances are due to constructive interference of the r_{212} reflected ray (the prompt reflection) and the first reflected ray having an r_{212} factor (the first delayed reflection).

The expanded form of the solution requires two additional comments. First, the interaction of an incoming wave with one of the interfaces is presumed to be independent of its interaction with the other interface. It does not depend on whether the other interface exists or not, or how far away it is. As pointed out in [17], if the details of the interaction of the wave with one of the interfaces depended in some way on the details of the second interface, the situation would belong to the realm of many-body theory rather than multiple scattering. Second, although the original differential equation (12) is in instantaneous form because all of its terms and the imposition of the boundary conditions are evaluated at the single time t , the expanded solution is an explicit representation of all the retardation effects that were hidden in the compact form of the solution (13a)–(13c).

The full physical implications of multiple scattering become apparent if a temporally-short pulse were incident on the well region, rather than a single monochromatic wave of infinite temporal duration. We assume that the incident plane wave pulse in region 1 is Gaussian in z , has unit height, amplitude $1/e$ half-width w_0 , dominant wave-number k_0 , and that the pulse's peak passes the origin at $t=0$ in the absence of the two interfaces,

$$\psi_{inc}(z, t) = \exp[ik_0(z-ct)] \exp[-(z-ct)^2/w_0^2]. \quad (19)$$

The Fourier spectrum of the pulse at $t=0$ is

$$\begin{aligned} A(k_1, 0) &= \int_{-\infty}^{\infty} dz \psi_{inc}(z, 0) \exp(-ik_1z) \\ &= \pi^{1/2} w_0 \exp[(k_1 - k_0)^2 w_0^2 / 4]. \end{aligned} \quad (20)$$

For $t > 0$ the spectrum is $A(k_1, 0) \exp[-i\omega(k_1)t]$, where $\omega(k_1)$ in the external regions is given by Eq. (10).

When the pulse is incident on the well region, the time dependence of the transmitted and reflected wave can be obtained using numerical finite-difference time-domain methods on the original partial differential equation (8) [30]. This method is well-suited for waves with a nonlinear dispersion relation, such as quantum mechanical waves or water waves. An alternative approach that has the pedagogic virtue of being exactly analytically soluble for waves with a linear dispersion relation and an incident

Gaussian pulse is to multiply the monochromatic frequency-domain solution by the time-dependent spectrum function of the pulse, and then take the inverse Fourier transform with respect to k_1 (see Sec. 11.2 of [23] and Sec. 15.8 of [20]). For example, we assume that the pulse of Eq. (19) in region 1 is incident on the well region from the left. Then

$$\psi_{ref}(z, t) = \int_{-\infty}^{\infty} \frac{dk_1}{2\pi} \psi_{ref}(k_1, z) \{A(k_1, 0) \exp[-i\omega(k_1)t]\} \exp[ik_1(-z)], \quad (21a)$$

$$\psi_{trans}(z, t) = \int_{-\infty}^{\infty} \frac{dk_1}{2\pi} \psi_3(k_1, z) \{A(k_1, 0) \exp[-i\omega(k_1)t]\} \exp(ik_1 z), \quad (21b)$$

where ψ_{ref} is the reflected portion of ψ_1 . Again ignoring the weak wavelength dependence of the Fresnel transmission and reflection coefficients,

$$t_{12} = 2/(N_2 + 1), \quad (22a)$$

$$t_{21} = 2N_2/(N_2 + 1), \quad (22b)$$

$$r_{212} = (N_2 - 1)/(N_2 + 1), \quad (22c)$$

$$r_{121} = -(N_2 - 1)/(N_2 + 1) \quad (22d)$$

are constants. The integral of the compact form (13a)–(13c) and (15a)–(15e) cannot be performed analytically because of the nonlinearity in k_1 of the denominator of the coefficients B and E . However, substituting Eqs. (18a) and (18c) for the expanded form, the Gaussian spectrum function (20), and $\exp(-ikct)$ corresponding to the linear dispersion relation (10) into Eqs. (21a) and (21b), the inverse Fourier transform can be performed analytically, giving the reflected wave as

$$\begin{aligned} \psi_{ref}(z, t) = & r_{121} \exp[-ik_0(z+ct)] \exp\left[-(z+ct)^2/w_0^2\right] \\ & + \sum_{n=1}^{\infty} t_{21}(r_{212})^{2n-1} t_{12} \exp[ik_0(z+ct+2nN_2L)] \\ & \times \exp\left[-(z+ct+2nN_2L)^2/w_0^2\right] \end{aligned} \quad (23a)$$

and the transmitted wave as

$$\begin{aligned} \psi_{trans}(z, t) = & \sum_{n=0}^{\infty} t_{21}(r_{212})^{2n} t_{12} \\ & \times \exp\{ik_0[z-L-ct+(2n+1)N_2L]\} \\ & \times \exp\left\{-[z-L-ct+(2n+1)N_2L]^2/w_0^2\right\}. \end{aligned} \quad (23b)$$

Eqs. (21a) and (21b) are equally valid for other spectrum functions, but the integrals involved may not be analytically soluble, opposite to the case for the incident Gaussian plane wave pulse (19).

Both the reflected wave (23a) and the transmitted wave (23b) are an infinite sequence of evenly-delayed Gaussian pulses of decreasing height resulting from the increasing number of internal reflection factors r_{212} . This is pictorially illustrated for the transmitted wave in Fig. 2. An observer at $z > L$ detects the peak of the n -th transmitted pulse at the time

$$t = (z-L)/c + (2n+1)N_2L/c, \quad (24a)$$

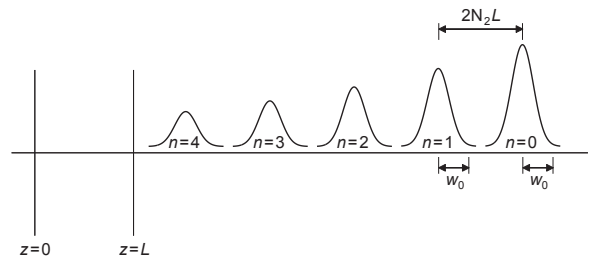


Fig. 2. Sequence of distinct transmitted pulses of Eq. (23b) when $w_0 < N_2L$.

and an observer at $z < 0$ detects the peak of the n -th reflected pulse at

$$t = (-z)/c + 2nN_2L/c. \quad (24b)$$

These time delays are exactly the time a ray would take to traverse the optical length of each multi-particle path in the expanded form of the frequency-domain problem. In the context of acoustics, the analog of Eqs. (23a) and (23b) in region 2, obtained from Eq. (18b), is familiar as the series of echoes one hears after clapping one's hands in a large, empty auditorium.

What the inverse Fourier transform (21a) and (21b) does is to essentially read the complicated spatial interference pattern of all the multi-particle paths in the frequency domain solution, and separate them into different time-delayed signals. Each transmitted pulse has a different overall phase with respect to the others, and would continue to spatially interfere with them if the incident pulse is suitably long and L is sufficiently small, i.e. $w_0 > N_2L$. However, it will not spatially overlap with them and a sequence of distinct transmitted pulses will result if the incident pulse is suitably short and L is sufficiently large, i.e. $w_0 < N_2L$. The same is true for the sequence of reflected pulses. A spatial analogy to this is a laser beam diagonally incident on a dielectric block having parallel interfaces. If the beam is wide and the angle of incidence on the block is near-normal, the different transmitted beams spatially overlap and interfere. But if the beam is narrow and the angle of incidence is steep, the transmitted beams no longer spatially overlap (see Fig. 4.55 of [31]). As long as $w_0 < N_2L$, the temporal sequence of distinct, non-interfering scattered pulses cannot be transformed away by writing the solution in a different form or by solving the original time-dependent differential equation using a different method. Their persistence is the hallmark of multiple scattering being a real physical process unfolding in time.

4. Isotropic scattering of a scalar wave by a collection of point-particles

This example is more complicated than the example of Section 3 because it is three-dimensional. It is, however, the simplest three-dimensional example of frequency-domain multiple scattering since the boundary conditions are applied only at the point-locations of the scattering particles (see [16] and pp. 765–766 of [12]). In spite of this example's geometric simplicity and lack of notational complexity, its solution fully illustrates the significant features of time-domain multiple scattering in three

dimensions. It is also the starting point in the derivation of the equations of diffusing wave spectroscopy [18,19].

Consider a collection of point-particles labeled by the subscript j , where $1 \leq j \leq N$ (not to be confused with the refractive index $N(z)$, N , or N_2 in the example of Section 3) at the known fixed positions \mathbf{r}_{j0} with respect to the origin. The coherent incident beam is a monochromatic scalar plane wave of wavelength λ , wave-vector \mathbf{k}_{inc} , angular frequency ω , and amplitude ψ_0 :

$$\psi_{beam}(\mathbf{r}_{p0}, t) = \psi_0 \exp(i\mathbf{k}_{inc} \cdot \mathbf{r}_{p0} - i\omega t), \quad (25)$$

where p is an arbitrary point in space whose position with respect to the origin is \mathbf{r}_{p0} . The radially outwardly-propagating spherical wave ψ_{scatt}^j created by the interaction of the incident beam with the point-particle j is

$$\psi_{scatt}^j(\mathbf{r}_{p0}, t) = -\frac{\exp(ikr_{pj})}{kr_{pj}} b^j \psi_{inc}^j(\mathbf{r}_{j0}, t), \quad (26)$$

where \mathbf{r}_{pj} is the position of point p with respect to the particle's point position. The form of the outgoing wave of Eq. (26) is valid both in the near-zone and far-zone. This will not be the case for the more complicated examples of the next few sections in which near-zone fields slowly evolve into far-zone fields. The right-most factor in Eq. (26) is the incident wave evaluated at the particle's point position, the middle factor is the dimensionless complex scattering amplitude $-b^j$, and the left-most factor is the dependence of the outgoing scattered spherical wave evaluated at p . The scattering amplitude contains an external minus sign here in order to conform to the notation of the examples of the next two sections. Also, the scattering amplitude $-b^j$ for point particles will not depend on k since there is no other quantity having the units of length describing the particle which can be combined with k in order to make the result dimensionless. The relation between the wave incident on j and the wave scattered by j is in general most conveniently written in the coordinate system centered on j . In Eq. (26), however, one encounters no ambiguity by writing it in the coordinate system centered on the origin because (i) the scattering object is a point-particle and (ii) the scattered wave is isotropic, i.e. there is no angle dependence to transform from one coordinate system to another.

We wish to express the dominant rapidly-varying k -dependent phase of the outgoing scattered wave with respect to origin's coordinate system. This is done in the following way. If the point p is sufficiently far from particle j so that $r_{p0} \gg r_{j0}$ and $2r_{p0} \gg kr_{j0}^2$ (i.e., the distance between p and j is in the Fraunhofer zone rather than in the closer Fresnel zone), one has

$$kr_{pj} = k|\mathbf{r}_{p0} - \mathbf{r}_{j0}| \approx k(r_{p0} - \mathbf{u}_{scatt} \cdot \mathbf{r}_{j0}), \quad (27)$$

where \mathbf{u}_{scatt} is a unit vector given by

$$\mathbf{u}_{scatt} \equiv \mathbf{r}_{p0} / r_{p0}. \quad (28)$$

Similarly we define the scattered wave-vector to the point p in the origin's coordinate system as

$$\mathbf{k}_{scatt} \equiv k\mathbf{u}_{scatt}. \quad (29)$$

The far-zone limit of the total wave, which is the sum of the incident beam plus the scattered wave as in Eq. (1),

then becomes for plane wave incidence

$$\begin{aligned} \psi_{total}(\mathbf{r}_{p0}, t) &\rightarrow \psi_0 \exp(i\mathbf{k}_{inc} \cdot \mathbf{r}_{p0} - i\omega t) \\ &\quad - \frac{\exp(ikr_{p0})}{kr_{p0}} \exp[i(\mathbf{k}_{inc} - \mathbf{k}_{scatt}) \cdot \mathbf{r}_{j0}] \\ &\quad \times b^j \psi_0 \exp(-i\omega t). \end{aligned} \quad (30)$$

The second k -dependent phase in the second term of Eq. (30) arises from evaluating the incident plane wave at the position of particle j , and the third phase comes from the far-zone limit of the wave scattered by j . The quantity $\mathbf{k}_{inc} - \mathbf{k}_{scatt}$ is often referred to as the scattered momentum transfer. As was mentioned in regard to Eq. (1), the specific form chosen for the total wave of Eq. (30) implies that the incident beam is not converted into the scattered wave by its interaction with the particle. Rather, the scattered wave is added to the incident beam everywhere in space.

For the case where there are N scattering particles, the total wave at \mathbf{r}_{p0} is the sum of the incident beam plus the wave scattered by each of the particles. Temporarily leaving the time dependence $\exp(-i\omega t)$ of each term implicit, we have

$$\psi_{total}(\mathbf{r}_{p0}) = \psi_{beam}(\mathbf{r}_{p0}) + \sum_{j=1}^N \psi_{scatt}^j(\mathbf{r}_{p0}). \quad (31)$$

The total wave in the far-zone for plane wave incidence is then

$$\begin{aligned} \psi_{total}(\mathbf{r}_{p0}) &\rightarrow \psi_0 \exp(i\mathbf{k}_{inc} \cdot \mathbf{r}_{p0}) \\ &\quad - \frac{\exp(ikr_{p0})}{kr_{p0}} \sum_{j=1}^N \exp(-i\mathbf{k}_{scatt} \cdot \mathbf{r}_{j0}) b^j \psi_{inc}^j(\mathbf{r}_{j0}). \end{aligned} \quad (32)$$

In addition, the wave incident on j is the sum of the incident beam and the waves scattered by all the other particles $i \neq j$,

$$\psi_{inc}^j(\mathbf{r}_{j0}) = \psi_{beam}(\mathbf{r}_{j0}) - \sum_{i=1}^N \frac{\exp(ikr_{ji})}{kr_{ji}} b^i \psi_{inc}^i(\mathbf{r}_{i0}), \quad (33)$$

where $r_{ji} = r_{ij}$ is the distance between particles j and i , which plays the role of the distance L between the 12 and 23 interfaces in the example of Section 3. The sum \sum_i^j denotes that the term $i=j$ is not included in the sum over i . Again, the right-most factor in the sum is the wave incident at the point-position of i , the middle factor is the dimensionless scattering amplitude of i , and the left-most factor is the dependence of the outgoing wave created at i evaluated at the point-position of j . Eq. (33) is a set of N algebraic equations coupled in particle number, that along with Eq. (32) are the compact form of the scattering equations.

In order to emphasize the idea of multi-particle paths in the frequency-domain, we again express the dominant k -dependent phase of each of the terms in Eqs. (32) and (33), considered in the far-zone, with respect to the origin's coordinate system. Using

$$\exp(ikr_{ji}) = \exp(i\mathbf{k}_{ji} \cdot \mathbf{r}_{ji}) = \exp[i\mathbf{k}_{ji} \cdot (\mathbf{r}_{j0} - \mathbf{r}_{i0})], \quad (34)$$

the wave incident on j of Eq. (33) becomes

$$\psi_{inc}^j(\mathbf{r}_{j0}) = \psi_0 \exp(i\mathbf{k}_{inc} \cdot \mathbf{r}_{j0}) - \sum_{i=1}^N \frac{1}{kr_{ji}} b^i \exp[i\mathbf{k}_{ji} \cdot (\mathbf{r}_{j0} - \mathbf{r}_{i0})] \psi_{inc}^i(\mathbf{r}_{i0}). \quad (35)$$

We assume the scattering amplitude b^i is small enough and the optical interparticle distance kr_{ji} is large enough so that iteration of Eq. (35) converges. The convergence criterion will be made more precise in Eq. (40) below. Then iterating Eq. (35) for plane wave incidence, and substituting the result into Eq. (32), we obtain the expanded form of the total wave in the far-zone

$$\begin{aligned} \psi_{total}(\mathbf{r}_{p0}) \rightarrow & \psi_0 \exp(i\mathbf{k}_{inc} \cdot \mathbf{r}_{p0}) \\ & - \frac{\exp(ikr_{p0})}{kr_{p0}} \sum_{j=1}^N b^j \exp[i(\mathbf{k}_{inc} - \mathbf{k}_{scatt}) \cdot \mathbf{r}_{j0}] \psi_0 \\ & + \frac{\exp(ikr_{p0})}{kr_{p0}} \sum_{j=1}^N \sum_{i=1}^N b^j \exp[i(\mathbf{k}_{ji} - \mathbf{k}_{scatt}) \cdot \mathbf{r}_{j0}] \\ & \times \frac{1}{kr_{ji}} b^i \exp[i(\mathbf{k}_{inc} - \mathbf{k}_{ji}) \cdot \mathbf{r}_{i0}] \psi_0 \\ & - \frac{\exp(ikr_{p0})}{kr_{p0}} \sum_{j=1}^N \sum_{i=1}^N \sum_{m=1}^N b^j \exp[i(\mathbf{k}_{ji} - \mathbf{k}_{scatt}) \cdot \mathbf{r}_{j0}] \\ & \times \frac{1}{kr_{ji}} b^i \exp[i(\mathbf{k}_{im} - \mathbf{k}_{ji}) \cdot \mathbf{r}_{i0}] \frac{1}{kr_{im}} b^m \\ & \times \exp[i(\mathbf{k}_{inc} - \mathbf{k}_{im}) \cdot \mathbf{r}_{m0}] \psi_0 + \dots \end{aligned} \quad (36)$$

The multi-particle paths implied in this version of the solution can be seen by reading the factors in each line of Eq. (36) corresponding to single, double, and triple

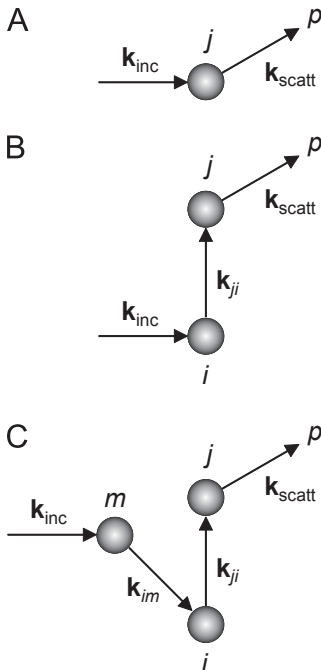


Fig. 3. Multiple-scattering paths of the second, third, and fourth terms of Eq. (36), corresponding to (a) single-scattering, (b) double-scattering, and (c) triple-scattering.

scattering, from right to left and comparing with Fig. 3a–c. The k -dependent phase of each term corresponds exactly to the optical length of each multiple-scattering path traversed by a ray.

In order to obtain an explicit solution to the compact form equations that can be discussed in detail, we consider the case of only two scattering particles i and j (see [10] and pp. 765–766 of [12]). Eq. (35) now reduces to a set of two coupled linear algebraic equations whose solution is

$$\psi_{inc}^j(\mathbf{r}_{j0}) = \{\exp(i\mathbf{k}_{inc} \cdot \mathbf{r}_{j0}) - (kr_{ji})^{-1} b^i \exp(i\mathbf{k}_{ji} \cdot \mathbf{r}_{j0})\} \times \exp[i(\mathbf{k}_{inc} - \mathbf{k}_{ji}) \cdot \mathbf{r}_{j0}] \psi_0 / G, \quad (37a)$$

$$\psi_{inc}^i(\mathbf{r}_{i0}) = \{\exp(i\mathbf{k}_{inc} \cdot \mathbf{r}_{i0}) - (kr_{ij})^{-1} b^j \exp(i\mathbf{k}_{ij} \cdot \mathbf{r}_{i0})\} \times \exp[i(\mathbf{k}_{inc} - \mathbf{k}_{ji}) \cdot \mathbf{r}_{j0}] \psi_0 / G \quad (37b)$$

with

$$G = 1 - \frac{b^i b^j}{(kr_{ji})^2} \exp[i(\mathbf{k}_{ji} - \mathbf{k}_{ij}) \cdot \mathbf{r}_{j0}] \exp[i(\mathbf{k}_{ij} - \mathbf{k}_{ji}) \cdot \mathbf{r}_{i0}]. \quad (38)$$

The total wave in the far-zone is then

$$\begin{aligned} \psi(\mathbf{r}_{p0}) \rightarrow & \psi_0 \exp(i\mathbf{k}_{inc} \cdot \mathbf{r}_{p0}) \\ & - \frac{\exp(ikr_{p0})}{kr_{p0}} \left[\exp(-i\mathbf{k}_{scatt} \cdot \mathbf{r}_{j0}) b^j \psi_{inc}^j(\mathbf{r}_{j0}) \right. \\ & \left. + \exp(-i\mathbf{k}_{scatt} \cdot \mathbf{r}_{i0}) b^i \psi_{inc}^i(\mathbf{r}_{i0}) \right]. \end{aligned} \quad (39)$$

Substituting Eqs. (37a), (37b), and (38) into Eq. (39), one obtains the compact form of the far-zone total wave. This is a convenient form of the solution if one wanted to numerically compute the scattered intensity at some set of polar and azimuth angles θ_{p0} and φ_{p0} . We assume that the scattering amplitude of each particle is sufficiently small and that the two particles are sufficiently far apart so that

$$\frac{b^i b^j}{(kr_{ji})^2} < 1, \quad (40)$$

the wave scattered from j to i and then from i back to j is weaker than the wave initially incident on j , i.e. multiple scattering is not an amplifier of the wave. In these circumstances the $1/G$ factor can be expanded as a geometric series. This is an analogy to the expansion of the denominator of Eqs. (15a)–(15d) in the one-dimensional example of Section 3, and also to the Debye series expansion of Lorenz–Mie theory where each partial wave scattering amplitude is re-expressed as a sum of an infinite number of terms interpreted in the $d^j \gg \lambda$ limit as diffraction, external reflection, and transmission following $q - 1$ internal reflections with $q \geq 1$ describing coherent multiple scattering inside a single particle [32–34]. The expanded form of Eq. (39) is then

$$\begin{aligned} \psi(\mathbf{r}_{p0}) \rightarrow & \psi_0 \exp(i\mathbf{k}_{inc} \cdot \mathbf{r}_{p0}) \\ & - \frac{\exp(ikr_{p0})}{kr_{p0}} b^j \exp(-i\mathbf{k}_{scatt} \cdot \mathbf{r}_{j0}) \\ & \times \left\{ \sum_{n=0}^{\infty} \left[\exp(i\mathbf{k}_{ji} \cdot \mathbf{r}_{j0}) (kr_{ji})^{-1} b^i \exp[i(\mathbf{k}_{ij} - \mathbf{k}_{ji}) \cdot \mathbf{r}_{i0}] \right. \right. \\ & \left. \left. \times (kr_{ij})^{-1} b^j \exp(-i\mathbf{k}_{ij} \cdot \mathbf{r}_{j0}) \right]^n \right\} \exp(i\mathbf{k}_{inc} \cdot \mathbf{r}_{j0}) \psi_0 \end{aligned}$$

$$\begin{aligned}
& + \frac{\exp(ikr_{p0})}{kr_{p0}} b^j \exp[i(\mathbf{k}_{ji} - \mathbf{k}_{scatt}) \cdot \mathbf{r}_{j0}] \\
& \times \left\{ \sum_{n=0}^{\infty} \left[(kr_{ji})^{-1} b^i \exp[i(\mathbf{k}_{ij} - \mathbf{k}_{ji}) \cdot \mathbf{r}_{j0}] (kr_{ij})^{-1} b^j \right. \right. \\
& \times \left. \left. \exp[i(\mathbf{k}_{ji} - \mathbf{k}_{ij}) \cdot \mathbf{r}_{j0}] \right]^n \right\} \\
& \times (kr_{ji})^{-1} b^i \exp[i(\mathbf{k}_{inc} - \mathbf{k}_{ji}) \cdot \mathbf{r}_{i0}] \psi_0 \\
& - \frac{\exp(ikr_{p0})}{kr_{p0}} b^j \exp(-i\mathbf{k}_{scatt} \cdot \mathbf{r}_{i0}) \left\{ \sum_{n=0}^{\infty} \left[\exp(i\mathbf{k}_{ij} \cdot \mathbf{r}_{i0}) (kr_{ij})^{-1} \right. \right. \\
& \times \left. \left. b^i \exp[i(\mathbf{k}_{ji} - \mathbf{k}_{ij}) \cdot \mathbf{r}_{j0}] (kr_{ji})^{-1} b^j \exp(-i\mathbf{k}_{ji} \cdot \mathbf{r}_{i0}) \right]^n \right\} \\
& \times \exp(i\mathbf{k}_{inc} \cdot \mathbf{r}_{i0}) \psi_0 \\
& + \frac{\exp(ikr_{p0})}{kr_{p0}} b^i \exp[i(\mathbf{k}_{ij} - \mathbf{k}_{scatt}) \cdot \mathbf{r}_{i0}] \\
& \times \left\{ \sum_{n=0}^{\infty} \left[(kr_{ij})^{-1} b^j \exp[i(\mathbf{k}_{ji} - \mathbf{k}_{ij}) \cdot \mathbf{r}_{j0}] (kr_{ji})^{-1} b^i \right. \right. \\
& \times \left. \left. \exp[i(\mathbf{k}_{ij} - \mathbf{k}_{ji}) \cdot \mathbf{r}_{j0}] \right]^n \right\} \\
& \times (kr_{ij})^{-1} b^j \exp[i(\mathbf{k}_{inc} - \mathbf{k}_{ij}) \cdot \mathbf{r}_{j0}] \psi_0. \quad (41)
\end{aligned}$$

The first term of Eq. (41) is the incident wave at the position of the far-zone detector. The second term may be interpreted using the multi-particle path point of view. Reading the factors from right to left, an incident wave strikes particle j and creates a scattered wave that propagates radially outward from j in all directions. It either reaches the detector directly ($n=0$), or it can scatter back and forth $n \geq 1$ times between particles i and j . A new radially outgoing scattered wave is created at each interaction, and eventually the wave created at particle j reaches the detector as well. This is pictorially illustrated in Fig. 4a. The third term may be interpreted as the incident wave striking particle i and

creating a scattered wave that propagates radially outward in all directions and is then scattered by particle j . The new wave propagating outward from j in all directions either reaches the detector directly ($n=0$), or it can scatter back and forth $n \geq 1$ times between particles i and j . Again a new radially outgoing scattered wave is created at each interaction, and eventually the wave created at particle j reaches the detector as well, as is illustrated in Fig. 4b. The interpretation of the fourth term is similar to that of the second, except that the incident wave is first scattered by particle i , the radially outgoing wave from i scatters back and forth between particles j and i , and eventually the wave created at i reaches the detector, as is illustrated in Fig. 4c. The interpretation of the fifth term is similar to that of the third term, except that the incident wave is first scattered by particle j . The radially outgoing wave from j propagates in all directions and is scattered at particle i . The scattered wave created there scatters back and forth between particles j and i , and eventually the radially outgoing wave from i reaches the detector, as is illustrated in Fig. 4d. The k -dependent phase of each of the terms again corresponds exactly to the optical length of each of the multi-particle paths involving the two scattering particles traversed by a ray. All the waves reaching the detector superpose there, and their interference produces a complicated intensity pattern at the detector plane. If the particles were moving as a function of time due to e.g. Brownian motion, the interference pattern produced at the detector plane would also change as a function of time. This change is the quantity measured in autocorrelation experiments in dynamic light scattering. It should also be mentioned that if the procedure of Eqs. (36) and (41) is applied to $N > 2$ scattering particles, the number of multi-particle paths quickly becomes very large as a function of N (see [35] for the analogous situation for scattering by a coated sphere).

Now consider the time-domain situation where a short time duration pulse, such as the Gaussian plane wave pulse of Eq. (19), is incident on particles i and j . The time-domain scattered wave is again obtained by multiplying Eq. (36) or Eq. (41) by the spectrum function of the incident plane wave pulse of Eq. (20), and by $\exp(-ikct)$ corresponding to the presumed linear dispersion relation of scalar waves in the external medium, and then performing the one-dimensional inverse Fourier transform with respect to k . We assume that the spectrum function of Eq. (20) is sufficiently narrow so that all the slowly varying k -dependence, such as the factors of $1/k$ in Eq. (41), can be approximately evaluated at k_0 , and the integral over only the dominant k -dependent phase terms remains. The inverse Fourier transform of the compact form cannot be obtained analytically because of the k -dependence of Eq. (38). But when Eq. (38) is expanded into an infinite geometric series as in Eq. (41), the inverse Fourier transform can be analytically evaluated term by term. The second term of Eq. (41) gives rise to a sequence of scattered Gaussian pulses whose center arrives at the detector at

$$t = (r_{p0} + \mathbf{u}_{inc} \cdot \mathbf{r}_{j0} - \mathbf{u}_{scatt} \cdot \mathbf{r}_{j0})/c + 2nr_{ji}/c. \quad (42a)$$

The third term gives rise to a sequence of scattered pulses detected at

$$t = (r_{p0} + \mathbf{u}_{inc} \cdot \mathbf{r}_{i0} - \mathbf{u}_{scatt} \cdot \mathbf{r}_{i0})/c + (2n+1)r_{ji}/c, \quad (42b)$$

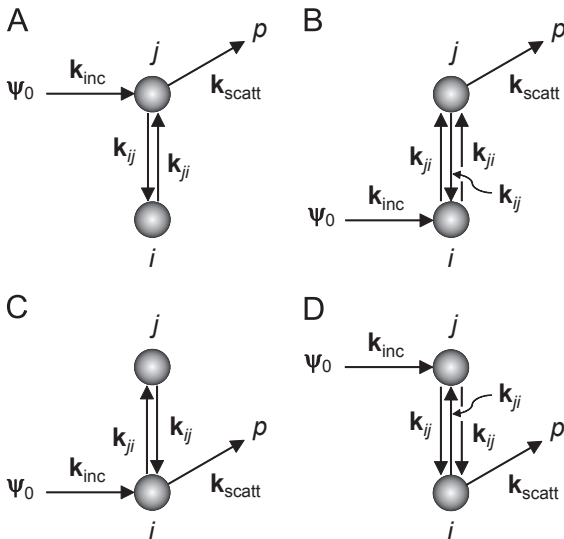


Fig. 4. Multiple-scattering paths of the (a) second, (b) third, (c) fourth, and (d) fifth terms of Eqs. (41) for $n=1$ for scattering by two point-particles i and j .

the fourth term gives a pulse sequence at

$$t = (r_{p0} + \mathbf{u}_{inc} \cdot \mathbf{r}_{i0} - \mathbf{u}_{scatt} \cdot \mathbf{r}_{i0})/c + 2nr_{ji}/c, \quad (42c)$$

and the fifth term gives

$$t = (r_{p0} + \mathbf{u}_{inc} \cdot \mathbf{r}_{j0} - \mathbf{u}_{scatt} \cdot \mathbf{r}_{i0})/c + (2n+1)r_{ji}/c. \quad (42d)$$

These delay times again are exactly the time a ray would take to traverse each of the frequency-domain multi-particle paths to the detector. In each case the temporal pulse separation within a sequence is

$$\Delta t = 2r_{ji}/c. \quad (43)$$

As long as $w_0 < r_{ji}$ the pulses do not spatially overlap and the complicated former interference pattern at the detector plane in the frequency-domain now is four sets of non-overlapping temporal pulse sequences. This is the signature of time-domain multiple scattering being a real physical process for this system. If the slow k -dependence, such as the increasing number of $1/k$ factors for higher order terms, cannot be closely approximated by its value at k_0 , it can be Taylor series expanded about k_0 , with the even terms of the expansion producing a distortion of the shape and a gradual spreading of the scattered pulses from the original Gaussian shape (see Sec. 7.4 of [36] and p. 67 of [37]). The distortion and spreading is expected to grow as n increases in Eq. (41). In the context of time-domain scattering by a single particle, however, it was found that this effect produced only a small broadening of the Debye series time-domain trajectories [38]. As an aside, it would be of interest to determine how Eqs. (42a)–(42d) could be used to determine \mathbf{r}_{i0} and \mathbf{r}_{j0} from experimental data, essentially performing a tomographic reconstruction of the scatterer configuration from the details of the observed pulse sequence.

It should be emphasized again that at each interaction of a wave with either particle i or j , a new scattered spherical wave is created that propagates radially outward in all directions from the particle. If it has propagated outward from j , sooner or later both particle i and the far-zone detector will be washed over by this spherical wave. The detector will then record the presence of the wave. But at particle i a new radially outgoing spherical wave will be created, and the resulting waves incident on the detector at different times will be recorded as the pulse sequence. Thus the multiple-scattering signal received at the detector is not analogous to that of a projectile particle bouncing back and forth between a number of fixed targets, as occurs for example in a pinball machine (see p. 29, Fig. 2.3 of [39]). Rather, the multiple scattering of waves is more analogous to a relay race in which a baton is passed from one runner to the next throughout the race. In this case the “baton” is the information that an incident pulse has washed over the particles. For example, in the fourth term of Eq. (36), the information about the incident pulse was encoded at the first scattering event into the amplitude and shape of the radially outgoing spherical wave created at particle m . When that wave washed over particle i , it passed the information on to the new radially outgoing spherical wave originating at i . When that wave washed over particle j , it again passed the information on to the new radially outgoing spherical wave originating at j . The detector reads the information carried by this last wave.

5. Scattering of a scalar wave by a collection of spherical particles of finite size

We now add a new level of complexity to the situation. The N scattering particles will no longer be fixed point-particles, but will be fixed homogeneous spheres of radius a^j . A consequence of this is that the boundary conditions for the wave equation must be satisfied at every point on the surface of the spherical particles rather than only at the point-positions as in the previous example. Further, we assume for the time-domain calculation that the particles are not in contact or near-contact with each other, but are spaced by at least a few diameters. The calculation of multiple scattering will proceed in a manner analogous to that of Section 4, but now it will contain the additional complexity of translating various quantities of interest from one coordinate system to another. We first consider frequency-domain scattering of an incident arbitrary monochromatic scalar wave beam of wave-number k as a function of the coordinate \mathbf{r}_{p0} with respect to a fixed origin. In order to take advantage of the spherical symmetry of the scatterers, the amplitude of the coherent beam is expressed as a sum of partial waves and azimuthal modes,

$$\psi_{beam}(\mathbf{r}_{p0}, t) = \sum_{n_0, m_0} \psi_0 B_{m_0, n_0} j_{n_0}(kr_{p0}) P_{n_0}^{m_0}(\cos \theta_{p0}) \times \exp(im_0 \varphi_{p0}) \exp(-i\omega t), \quad (44)$$

where, as before, the angles θ_{p0} and φ_{p0} are the spherical coordinate angles with respect to the origin, j_n are spherical Bessel functions, P_n^m are associated Legendre functions, B_{m_0, n_0} are the dimensionless shape coefficients of the incident beam with respect to the origin's coordinate system, and \sum_{n_0, m_0} is the double sum over partial waves n_0 and azimuthal modes m_0 for $0 \leq n_0 < \infty$ and $-n_0 \leq m_0 \leq n_0$. If the incident scalar beam is a plane wave traveling in the $+z$ direction,

$$\psi_{beam}(\mathbf{r}_{p0}, t) = \psi_0 \exp(i\mathbf{k}_{inc} \cdot \mathbf{r}_{p0} - i\omega t) \quad (45)$$

with

$$\mathbf{k}_{inc} = k\mathbf{u}_z, \quad (46)$$

then the shape coefficients of this beam are

$$B_{m_0, n_0} = i^{n_0} (2n_0 + 1) \delta_{m_0, 0} \equiv (PW)_{m_0, n_0}, \quad (47)$$

where δ_{mn} is the Kronecker delta.

Particle j has its center at the position \mathbf{r}_{j0} with respect to the origin. Since the solutions of the scalar Helmholtz equation with respect to a given coordinate system form a complete set of functions, any function with respect to the origin can be written in terms of the solutions of the scalar Helmholtz equation with respect to a coordinate system centered on particle j whose axes are parallel to those of the origin's coordinate system. In particular,

$$j_{n_0}(kr_{p0}) P_{n_0}^{m_0}(\cos \theta_{p0}) \exp(im_0 \varphi_{p0}) = \sum_{n_j, m_j} J_{m_0, n_0; m_j, n_j}(\mathbf{r}_{j0}) j_{n_j}(kr_{pj}) \times P_{n_j}^{m_j}(\cos \theta_{pj}) \exp(im_j \varphi_{pj}), \quad (48)$$

where $J_{m_0, n_0; m_j, n_j}(\mathbf{r}_{j0})$ are a set of translation coefficients for scalar standing waves expressed in spherical coordinates [40–42]. Thus the incident beam of Eq. (44) can be written

with respect to the coordinate system centered on particle j as

$$\psi_{beam}(\mathbf{r}_{pj}, t) = \sum_{n_j, m_j} B_{m_j, n_j} \psi_0 j_{n_j}(kr_{pj}) P_{n_j}^{m_j}(\cos \theta_{pj}) \times \exp(im_j \varphi_{pj}) \exp(-i\omega t), \quad (49)$$

where the new shape coefficients B_{m_j, n_j} describe the beam with respect to the coordinate system centered on j . They are related to the original beam shape coefficients by

$$B_{m_j, n_j} = \sum_{n_0, m_0} B_{m_0, n_0} J_{m_0, n_0, m_j, n_j}(\mathbf{r}_{j0}). \quad (50)$$

In the coordinate system centered on particle j , the plane wave of Eqs. (44)–(47) is given by

$$\begin{aligned} \psi_{beam}(\mathbf{r}_{pj}, t) &= \psi_0 \exp[i\mathbf{k}_{inc} \cdot (\mathbf{r}_{pj} + \mathbf{r}_{j0}) - i\omega t] \\ &= \psi_0 \exp(i\mathbf{k}_{inc} \cdot \mathbf{r}_{j0}) \sum_{n_j, m_j} (PW)_{m_j, n_j} j_{n_j}(kr_{pj}) \\ &\quad \times P_{n_j}^{m_j}(\cos \theta_{pj}) \exp(im_j \varphi_{pj}) \exp(-i\omega t) \end{aligned} \quad (51)$$

since $\exp(i\mathbf{k}_{inc} \cdot \mathbf{r}_{pj})$ has the same functional form in the coordinate system of j as that $\exp(i\mathbf{k}_{inc} \cdot \mathbf{r}_{p0})$ had in the coordinate system centered on the origin.

The reason why the incident beam must be transformed from the coordinate system centered on the origin to the coordinate system centered on particle j is because when expressed as a sum over partial waves and azimuthal modes, the relation between the beam incident on j and the wave scattered by j is most naturally and conveniently described in the coordinate system centered on j . One has

$$\begin{aligned} \psi_{scatt}^j(\mathbf{r}_{pj}, t) &= - \sum_{n_j, m_j} b_{n_j}^j \psi_0 B_{m_j, n_j} h_{n_j}^{(1)}(kr_{pj}) \\ &\quad \times P_{n_j}^{m_j}(\cos \theta_{pj}) \exp(im_j \varphi_{pj}) \exp(-i\omega t), \end{aligned} \quad (52)$$

where $h_{n_j}^{(1)}$ are outgoing spherical Hankel functions and $b_{n_j}^j$ are the dimensionless partial wave scattering amplitudes of particle j if its center had been at the origin and a plane wave were incident on it. The partial wave scattering amplitudes are a function of ka^j (see Sec. 9.22 of [13]).

Eq. (52) requires a few comments. The specific form of $b_{n_j}^j$ results from matching the boundary conditions over the surface of particle j . For isotropic scattering in Eq. (26), the feature of the incident beam that the wave scattered by j directly depended on was $\psi_{inc}^j(\mathbf{r}_{j0}, t)$. But when particle j has radius $a^j > 0$, the wave scattered by j directly depends on the shape coefficients B_{m_j, n_j} of the incident beam [43]. Also since the particles have radius $a^j > 0$, the outgoing scattered wave of Eq. (52) is no longer isotropic, but depends on θ_{pj} and φ_{pj} . The isotropic scattering of Section 4 is the $n_j=0, m_j=0$ limit of Eq. (52).

If the detector is in the far-zone of particle j and is sufficiently far from the origin so that $r_{p0} \gg r_{j0}$ and $2r_{p0} \gg kr_{j0}^2$ then it is in the origin-centered far-zone of particle j as well, and we have [44–46]

$$h_{n_j}^{(1)}(kr_{pj}) \rightarrow (-i)^{n_j+1} \frac{\exp(ikr_{pj})}{kr_{pj}}, \quad (53a)$$

$$kr_{pj} \approx kr_{p0} - \mathbf{k}_{scatt} \cdot \mathbf{r}_{j0}, \quad (53b)$$

$$\theta_{pj} \approx \theta_{p0}. \quad (53c)$$

$$\varphi_{pj} \approx \varphi_{p0}. \quad (53d)$$

For plane wave incidence and with the $\exp(-i\omega t)$ time dependence temporarily left implicit, the total wave in the origin-centered far-zone becomes

$$\begin{aligned} \psi_{total}(\mathbf{r}_{p0}) &\rightarrow \psi_0 \exp(i\mathbf{k}_{inc} \cdot \mathbf{r}_{p0}) \\ &\quad - \frac{\exp(ikr_{p0})}{kr_{p0}} \exp[i(\mathbf{k}_{inc} - \mathbf{k}_{scatt}) \cdot \mathbf{r}_{j0}] \\ &\quad \times \sum_{n_j, m_j} b_{n_j}^j \psi_0 (PW)_{m_j, n_j} (-i)^{n_j+1} \\ &\quad \times P_{n_j}^{m_j}(\cos \theta_{p0}) \exp(im_j \varphi_{p0}). \end{aligned} \quad (54)$$

Again the second k -dependent phase in the second term arises from evaluating the incident plane wave at the center of particle j , and the third k -dependent phase arises from the origin-centered far-zone limit of the wave scattered by j .

As was the case in Eq. (31) of Section 4, when a beam is incident on a collection of N particles, the total wave at the detector is the sum of the incident beam plus the wave scattered by each of the particles. In the origin-centered far-zone this becomes

$$\begin{aligned} \psi_{total}(\mathbf{r}_{p0}) &\rightarrow \psi_0 \exp(i\mathbf{k}_{inc} \cdot \mathbf{r}_{p0}) \\ &\quad - \frac{\exp(ikr_{p0})}{kr_{p0}} \sum_{j=1}^N \exp(-i\mathbf{k}_{scatt} \cdot \mathbf{r}_{j0}) \\ &\quad \times \sum_{n_j, m_j} b_{n_j}^j \psi_0 B_{m_j, n_j} (-i)^{n_j+1} \\ &\quad \times P_{n_j}^{m_j}(\cos \theta_{p0}) \exp(im_j \varphi_{p0}). \end{aligned} \quad (55)$$

Similarly, the total wave incident on particle j is the sum of the incident plane wave and the waves scattered by each of the other particles $i \neq j$. However, according to Eq. (52) the wave scattered by i must be transformed from the coordinate system centered on i to the coordinate system centered on j so that its interaction with j can be expressed in terms of partial waves and azimuthal modes. This is accomplished using a second set of Helmholtz solution translation coefficients [40–42]

$$\begin{aligned} h_{n_i}^{(1)}(kr_{pi}) P_{n_i}^{m_i}(\cos \theta_{pi}) \exp(im_i \varphi_{pi}) \\ = \sum_{n_j, m_j} H_{m_i, n_i; m_j, n_j}(\mathbf{r}_{ji}) j_{n_j}(kr_{pj}) \\ \times P_{n_j}^{m_j}(\cos \theta_{pj}) \exp(im_j \varphi_{pj}), \end{aligned} \quad (56)$$

which is valid as long as $r_{pj} < r_{ji}$. This is always true for the wave scattered by i and incident on j because r_{pj} is evaluated on the surface of j where the boundary conditions are imposed. Using Eq. (56), the field scattered by particle i expressed in terms of the coordinate system centered on j becomes

$$\begin{aligned} \psi_{scatt}^i(\mathbf{r}_{pj}) &= - \sum_{n_j, m_j} \left[\sum_{n_i, m_i} b_{n_i}^i \psi_0 B_{m_i, n_i} H_{m_i, n_i; m_j, n_j}(\mathbf{r}_{ji}) \right] \\ &\quad \times j_{n_j}(kr_{pj}) P_{n_j}^{m_j}(\cos \theta_{pj}) \exp(im_j \varphi_{pj}). \end{aligned} \quad (57)$$

In order to obtain the shape coefficients of the total wave incident on particle j , we add to Eq. (57) the shape coefficients of Eq. (51) for an incident plane wave expressed in j 's coordinate system, giving the set of

coupled algebraic equations

$$B_{m_j, n_j} = \exp(i\mathbf{k}_{inc} \cdot \mathbf{r}_{j0})(PW)_{m_j, n_j} - \sum_{i=1}^N \sum_{n_i, m_i} b_{n_i}^i B_{m_i, n_i} H_{m_i, n_i; m_j, n_j}(\mathbf{r}_{ji}). \quad (58)$$

The shape coefficients are now coupled with respect to particle number, partial wave number, and azimuthal mode number. The fact that the coupled equations are algebraic in form results from our use of partial wave expansions that take advantage of the spherical symmetry of the scatterers. This will not be the case in Section 7 when we consider scatterers of arbitrary shape. Eqs. (55) and (58) are the compact form of the multiple-scattering equations for this situation. As was the case in Eq. (35) for point-particles, if Eq. (58) were iterated, one would obtain the equations in expanded form.

In order to separate out the dominant rapidly-varying k -dependent phase of each of the terms in Eqs. (55) and (58) so as to emphasize the multi-particle path interpretation in the frequency-domain, the collection of particles in question must be tenuous, such as water droplets in a cloud, rather than being touching or close-packed as would be the case for aggregated systems. Geometrically, the length of a vector from any point in particle j to any point in another particle i must differ by only a small percentage of their center-to-center distance, and the difference must also be small compared to the wavelength. If the particles are large and are touching, the percentage difference is quite large, and the approximation of Eq. (59) below will not be valid. Analytically, this geometrical argument is equivalent to the following. The explicit form of $H_{m_i, n_i; m_j, n_j}(\mathbf{r}_{ji})$ contains a sum over q , where the triangle inequality for the decomposition of the product of representations of the rotation group gives $|n_j - n_i| \leq q \leq n_j + n_i$. Each term of the sum over q contains a number of factors multiplied together, including $h_q^{(1)}(kr_{ji})$. When $kr_{ji} \gg q + 1/2 \gg 1$, or equivalently when the separation between the centers of the two spheres is much larger than when they are touching, $r_{ji} \gg a^j + a^i$, the outgoing spherical Hankel function has the far-zone limit

$$h_q^{(1)}(kr_{ji}) \rightarrow (-i)^{q+1} \frac{\exp(ikr_{ji})}{kr_{ji}} = (-i)^{q+1} \frac{\exp(i\mathbf{k}_{ji} \cdot \mathbf{r}_{ji})}{kr_{ji}} = (-i)^{q+1} \frac{\exp[i\mathbf{k}_{ji} \cdot (\mathbf{r}_{j0} - \mathbf{r}_{i0})]}{kr_{ji}}. \quad (59)$$

In order to obtain a more precise estimate of the value of r_{ji} for which this is valid for particles large with respect to the wavelength, we use Debye's asymptotic expansion of Bessel and Neumann functions near the transition region (see Sec. 9.3 of [47]). The approximation of Eq. (59) is then found to be reasonably accurate for

$$r_{ji} > 2(a^j + a^i), \quad (60)$$

or a volume fraction $f < 0.01$. For particles small compared to λ , the volume fraction can be somewhat higher [48].

In order to illustrate the importance of these rapidly-varying k -dependent phases for the multi-particle path interpretation in the frequency-domain, we consider the analog of one of the terms described in the example of Section 4. As was the case in Eq. (40), we again assume

that the partial wave scattering amplitudes are small enough and the distance between particles is large enough so that the iteration series of Eq. (58) converges. This is expected to be true as long as morphology-dependent resonances of the spheres are not excited [24,25,49]. In that situation, a resonance in the partial wave n_j of particle j may feed a substantial fraction of its energy into a neighboring sphere i , causing it to resonate in the partial wave n_i . If a substantial fraction of the energy of the resonance of sphere i feeds back into the resonance of sphere j , a positive feedback loop can be set up whose continuing amplification can cause the iteration series to diverge for those partial waves. This is the analog of Eq. (40) being violated for point-particle scattering. Assuming that this is not the case and the iteration series converges, the second order iteration of Eq. (58), when substituted into Eq. (55), is interpreted as the incident beam being scattered by particle m . The scattered outgoing spherical wave created there washes over particle i creating a new scattered wave. This new outgoing spherical wave washes over particle j , and the scattered wave created at j is recorded by the detector at point p . This m - i - j path contains the dominant rapidly-varying k -dependent phases

$$\exp[i(\mathbf{k}_{ji} - \mathbf{k}_{scat}) \cdot \mathbf{r}_{j0}] \exp[i(\mathbf{k}_{im} - \mathbf{k}_{ji}) \cdot \mathbf{r}_{i0}] \exp[i(\mathbf{k}_{inc} - \mathbf{k}_{im}) \cdot \mathbf{r}_{m0}]. \quad (61)$$

The fifth phase in Eq. (61) results from the incident beam evaluated at the position of particle m , the third and sixth phases result from the translation coefficient from m to i , the first and fourth phases result from the translation coefficients from i to j , and the second phase results from the far-zone limit of the wave scattered by j . In addition, there is slowly varying k -dependence in the $1/k$ factors and in the partial wave scattering amplitudes.

Instead of a plane wave of infinite temporal extent, let us now consider the case of a temporally-short Gaussian plane wave pulse incident on the collection of particles that are all in the far-zones of each other, as was specified in Eq. (60). This m - i - j path term is multiplied by the pulse spectrum function of Eq. (20) and $\exp(-ikct)$ corresponding to a linear dispersion relation for the scalar waves in the external medium. It is then inverse Fourier transformed with respect to k , and gives rise to a multiply-scattered pulse. The center of this pulse arrives at the detector at the time

$$t = (r_{p0} + \mathbf{u}_{inc} \cdot \mathbf{r}_{m0} + r_{im} + r_{ji} - \mathbf{u}_{scat} \cdot \mathbf{r}_{j0})/c. \quad (62)$$

Again each multi-particle path in frequency-domain multiple scattering is associated with a multiply-scattered pulse in time-domain multiple scattering. If the pulses are sufficiently narrow and the separation between the particles is sufficiently great, a sequence of temporally non-overlapping pulses is recorded by the detector. If the rapidly-varying k -dependent phases in the Debye series decomposition of the partial wave scattering amplitudes for each individual scattering were explicitly considered as well, each pulse in the sequence described above would contain a number of closely-spaced sub-pulses corresponding to diffraction, external reflection, transmission, etc. within each particle. These would act as a fine-structure superimposed on the results of Eq. (62). After a suitably large number of single particle interactions,

the time-delayed fine-structure of a scattered pulse corresponding to many internal reflections will start to overlap the prompt portion of the following pulse. But this will likely be a background effect since the strengths of the pulses corresponding to a large number of single-particle scatterings are small compared with that of pulses corresponding to only a few single-particle scatterings.

6. Scattering of an electromagnetic wave by a collection of spherical particles of finite size

We now add yet another level of complexity to the situation. The incident beam is no longer a scalar wave. Rather, it is an electromagnetic wave with a specified polarization state. The consequence of this is that one must now keep track of the transverse electric (TE) and transverse magnetic (TM) linear polarization components of the scattered light, and polarization-preserving and polarization-changing scattering amplitudes. Calculation of multiple scattering will proceed in a manner analogous to that of Section 5, but now there will be two sets of beam shape coefficients, rather than only one, and four sets of translation coefficients, rather than only two. The basis set of functions that the incident and scattered fields will be expanded in terms of are the dimensionless vector spherical wave functions $\mathbf{M}_{m,n}^{(K)}(\mathbf{kr})$ and $\mathbf{N}_{m,n}^{(K)}(\mathbf{kr})$ (see [50] and Appendix C of [51]), where $K=1$ indicates that the radial dependence is a spherical Bessel function and $K=3$ indicates that it is an outgoing spherical Hankel function. An arbitrary coherent incident beam in the coordinate system centered at the origin is

$$\mathbf{E}_{beam}(\mathbf{r}_{p0}, t) = E_0 \sum_{n_0, m_0} [p_{m_0, n_0} \mathbf{N}_{m_0, n_0}^{(1)}(\mathbf{kr}_{p0}) + q_{m_0, n_0} \mathbf{M}_{m_0, n_0}^{(1)}(\mathbf{kr}_{p0})] \exp(-i\omega t), \quad (63a)$$

$$\mathbf{cB}_{beam}(\mathbf{r}_{p0}, t) = E_0 \sum_{n_0, m_0} [q_{m_0, n_0} \mathbf{N}_{m_0, n_0}^{(1)}(\mathbf{kr}_{p0}) + p_{m_0, n_0} \mathbf{M}_{m_0, n_0}^{(1)}(\mathbf{kr}_{p0})] \exp(-i\omega t), \quad (63b)$$

where p_{m_0, n_0} and q_{m_0, n_0} are the dimensionless TM and TE shape coefficients of the beam, and \sum_{n_0, m_0} is now the double sum over $1 \leq n_0 < \infty$ and $-n_0 \leq m_0 \leq n_0$ since the $n_0 = m_0 = 0$ term of Section 5 does not occur for electromagnetic scattering. If the incident beam is an x -polarized plane wave traveling in the $+z$ direction, the shape coefficients with respect to the origin's coordinate system simplify to

$$p_{m_0, n_0} = q_{m_0, n_0} = -i^{n_0} \frac{2n_0 + 1}{2n_0(n_0 + 1)} \delta_{m_0, \pm 1} \equiv (PW)_{m_0, n_0}. \quad (64)$$

In analogy to Section 5, a vector spherical wave function with respect to a coordinate system centered on the origin can be written as a sum over vector spherical wave functions with respect to a coordinate system centered on particle j . In particular

$$\mathbf{M}_{m_0, n_0}^{(1)}(\mathbf{kr}_{p0}) = \sum_{n_j, m_j} [A_{m_0, n_0; m_j, n_j}^J(\mathbf{r}_{j0}) \mathbf{M}_{m_j, n_j}^{(1)}(\mathbf{kr}_{pj}) + B_{m_0, n_0; m_j, n_j}^J(\mathbf{r}_{j0}) \mathbf{N}_{m_j, n_j}^{(1)}(\mathbf{kr}_{pj})], \quad (65a)$$

$$\mathbf{N}_{m_0, n_0}^{(1)}(\mathbf{kr}_{p0}) = \sum_{n_j, m_j} [B_{m_0, n_0; m_j, n_j}^J(\mathbf{r}_{j0}) \mathbf{M}_{m_j, n_j}^{(1)}(\mathbf{kr}_{pj}) + A_{m_0, n_0; m_j, n_j}^J(\mathbf{r}_{j0}) \mathbf{N}_{m_j, n_j}^{(1)}(\mathbf{kr}_{pj})], \quad (65b)$$

where $A_{m_0, n_0; m_j, n_j}^J(\mathbf{r}_{j0})$ and $B_{m_0, n_0; m_j, n_j}^J(\mathbf{r}_{j0})$ are vector spherical wave function translation coefficients [40–42]. The incident beam of Eqs. (63a) and (63b) can be written in terms of the coordinate system centered on particle j as

$$\mathbf{E}_{beam}(\mathbf{r}_{pj}, t) = E_0 \sum_{n_j, m_j} [p_{m_j, n_j} \mathbf{N}_{m_j, n_j}^{(1)}(\mathbf{kr}_{pj}) + q_{m_j, n_j} \mathbf{M}_{m_j, n_j}^{(1)}(\mathbf{kr}_{pj})] \exp(-i\omega t), \quad (66a)$$

$$\mathbf{cB}_{beam}(\mathbf{r}_{pj}, t) = E_0 \sum_{n_j, m_j} [q_{m_j, n_j} \mathbf{N}_{m_j, n_j}^{(1)}(\mathbf{kr}_{pj}) + p_{m_j, n_j} \mathbf{M}_{m_j, n_j}^{(1)}(\mathbf{kr}_{pj})] \exp(-i\omega t), \quad (66b)$$

where

$$q_{m_j, n_j} = \sum_{n_0, m_0} [q_{m_0, n_0} A_{m_0, n_0; m_j, n_j}^J(\mathbf{r}_{j0}) + p_{m_0, n_0} B_{m_0, n_0; m_j, n_j}^J(\mathbf{r}_{j0})], \quad (67a)$$

$$p_{m_j, n_j} = \sum_{n_0, m_0} [q_{m_0, n_0} B_{m_0, n_0; m_j, n_j}^J(\mathbf{r}_{j0}) + p_{m_0, n_0} A_{m_0, n_0; m_j, n_j}^J(\mathbf{r}_{j0})]. \quad (67b)$$

The coefficients of the plane wave of Eq. (64) with respect to the coordinate system centered on particle j are

$$p_{m_j, n_j} = q_{m_j, n_j} = \exp(i\mathbf{k}_{inc} \cdot \mathbf{r}_{j0}) (PW)_{m_j, n_j}. \quad (68)$$

Again, scattering of the electromagnetic beam by the spherical particle j is most naturally and conveniently described when both the incident beam and the scattered fields are written in terms of the coordinate system centered on j ,

$$\mathbf{E}_{scatt}^j(\mathbf{r}_{pj}, t) = - \sum_{n_j, m_j} [a_{n_j}^j p_{m_j, n_j} \mathbf{N}_{m_j, n_j}^{(3)}(\mathbf{kr}_{pj}) + b_{n_j}^j q_{m_j, n_j} \mathbf{M}_{m_j, n_j}^{(3)}(\mathbf{kr}_{pj})] \exp(-i\omega t), \quad (69a)$$

$$\mathbf{cB}_{scatt}^j(\mathbf{r}_{pj}, t) = - \sum_{n_j, m_j} [a_{n_j}^j p_{m_j, n_j} \mathbf{M}_{m_j, n_j}^{(3)}(\mathbf{kr}_{pj}) + b_{n_j}^j q_{m_j, n_j} \mathbf{N}_{m_j, n_j}^{(3)}(\mathbf{kr}_{pj})] \exp(-i\omega t), \quad (69b)$$

where $a_{n_j}^j$ and $b_{n_j}^j$ are the Lorenz–Mie theory dimensionless TM and TE partial wave scattering amplitudes of particle j if the center of the particle were at the origin and an x -polarized plane wave traveling in the $+z$ direction were incident on it (see Sec. 9.22 of Ref. [13]). Again the fields scattered by j directly depend on the shape coefficients of the fields incident on j [43].

The total field in the exterior region is again the sum of the incident beam fields and the fields scattered by particle j [44–46]. For an x -polarized incident plane wave propagating in the $+z$ direction, using Eqs. (69a) and (69b) and temporarily leaving the $\exp(-i\omega t)$ time dependence implicit, one obtains in the origin-centered far-zone of j

$$\mathbf{E}_{total}(\mathbf{r}_{p0}) \rightarrow \mathbf{u}_x E_0 \exp(i\mathbf{k}_{inc} \cdot \mathbf{r}_{p0}) - \exp[i(\mathbf{k}_{inc} - \mathbf{k}_{scatt}) \cdot \mathbf{r}_{j0}]$$

$$\times \sum_{n_j, m_j} \left[a_{n_j}^j (PW)_{m_j, n_j} \mathbf{N}_{m_j, n_j}^{(3)}(\mathbf{k}\mathbf{r}_{p0}) + b_{n_j}^j q_{m_j, n_j} A_{m_j, n_j; m_j, n_j}^H(\mathbf{r}_{ji}) \right]. \quad (73b)$$

$$+ b_{n_j}^j (PW)_{m_j, n_j} \mathbf{M}_{m_j, n_j}^{(3)}(\mathbf{k}\mathbf{r}_{p0}) \Big] E_0, \quad (70a)$$

$$\begin{aligned} c\mathbf{B}_{total}(\mathbf{r}_{p0}) &\rightarrow \mathbf{u}_y E_0 \exp(i\mathbf{k}_{inc} \cdot \mathbf{r}_{p0}) \\ &- \exp[i(\mathbf{k}_{inc} - \mathbf{k}_{scatt}) \cdot \mathbf{r}_{j0}] \\ &\times \sum_{n_j, m_j} \left[a_{n_j}^j (PW)_{m_j, n_j} \mathbf{M}_{m_j, n_j}^{(3)}(\mathbf{k}\mathbf{r}_{p0}) \right. \\ &\left. + b_{n_j}^j (PW)_{m_j, n_j} \mathbf{N}_{m_j, n_j}^{(3)}(\mathbf{k}\mathbf{r}_{p0}) \right] E_0. \end{aligned} \quad (70b)$$

For an electromagnetic plane wave incident on a collection of N particles, the total far-zone fields are

$$\begin{aligned} \mathbf{E}_{total}(\mathbf{r}_{p0}) &\rightarrow \mathbf{u}_x E_0 \exp(i\mathbf{k}_{inc} \cdot \mathbf{r}_{p0}) \\ &- \sum_{j=1}^N \exp(-i\mathbf{k}_{scatt} \cdot \mathbf{r}_{j0}) \\ &\times \sum_{n_j, m_j} \left[a_{n_j}^j p_{m_j, n_j} \mathbf{N}_{m_j, n_j}^{(3)}(\mathbf{k}\mathbf{r}_{p0}) + b_{n_j}^j q_{m_j, n_j} \mathbf{M}_{m_j, n_j}^{(3)}(\mathbf{k}\mathbf{r}_{p0}) \right] E_0, \end{aligned} \quad (71a)$$

$$\begin{aligned} c\mathbf{B}_{total}(\mathbf{r}_{p0}) &\rightarrow \mathbf{u}_y E_0 \exp(i\mathbf{k}_{inc} \cdot \mathbf{r}_{p0}) \\ &- \sum_{j=1}^N \exp(-i\mathbf{k}_{scatt} \cdot \mathbf{r}_{j0}) \\ &\times \sum_{n_j, m_j} \left[a_{n_j}^j p_{m_j, n_j} \mathbf{M}_{m_j, n_j}^{(3)}(\mathbf{k}\mathbf{r}_{p0}) + b_{n_j}^j q_{m_j, n_j} \mathbf{N}_{m_j, n_j}^{(3)}(\mathbf{k}\mathbf{r}_{p0}) \right] E_0. \end{aligned} \quad (71b)$$

Similarly, the total fields incident on particle j are the sum of the incident beam fields and the fields scattered by each of the other particles $i \neq j$. Transforming the fields scattered by particle i from the coordinate system centered on i to the coordinate system centered on j is accomplished using a second set of vector spherical wave function translation coefficients [40–42]

$$\begin{aligned} \mathbf{M}_{m_i, n_i}^{(3)}(\mathbf{k}\mathbf{r}_{pi}) &= \sum_{n_j, m_j} [A_{m_i, n_i; m_j, n_j}^H(\mathbf{r}_{ji}) \mathbf{M}_{m_j, n_j}^{(1)}(\mathbf{k}\mathbf{r}_{pj}) \\ &+ B_{m_i, n_i; m_j, n_j}^H(\mathbf{r}_{ji}) \mathbf{N}_{m_j, n_j}^{(1)}(\mathbf{k}\mathbf{r}_{pj})], \end{aligned} \quad (72a)$$

$$\begin{aligned} \mathbf{N}_{m_i, n_i}^{(3)}(\mathbf{k}\mathbf{r}_{pi}) &= \sum_{n_j, m_j} [B_{m_i, n_i; m_j, n_j}^H(\mathbf{r}_{ji}) \mathbf{M}_{m_j, n_j}^{(1)}(\mathbf{k}\mathbf{r}_{pj}) \\ &+ A_{m_i, n_i; m_j, n_j}^H(\mathbf{r}_{ji}) \mathbf{N}_{m_j, n_j}^{(1)}(\mathbf{k}\mathbf{r}_{pj})] \end{aligned} \quad (72b)$$

as long as $r_{pj} < r_{ji}$, which is always the case here, for the reason mentioned in Section 5. The shape coefficients of the total fields incident on particle j expressed in the coordinate system centered on j for plane wave incidence are then given by

$$\begin{aligned} p_{m_j, n_j} &= \exp(i\mathbf{k}_{inc} \cdot \mathbf{r}_{j0}) (PW)_{m_j, n_j} \\ &- \sum_{i=1}^N \sum_{n_i, m_i} \left[a_{n_i}^i p_{m_i, n_i} A_{m_i, n_i; m_j, n_j}^H(\mathbf{r}_{ji}) \right. \\ &\left. + b_{n_i}^i q_{m_i, n_i} B_{m_i, n_i; m_j, n_j}^H(\mathbf{r}_{ji}) \right], \end{aligned} \quad (73a)$$

$$\begin{aligned} q_{m_j, n_j} &= \exp(i\mathbf{k}_{inc} \cdot \mathbf{r}_{j0}) (PW)_{m_j, n_j} \\ &- \sum_{i=1}^N \sum_{n_i, m_i} \left[a_{n_i}^i p_{m_i, n_i} B_{m_i, n_i; m_j, n_j}^H(\mathbf{r}_{ji}) \right. \end{aligned}$$

These form a very large set of algebraic equations, now coupled in particle number, partial wave number, azimuthal mode number, and polarization state. Eqs. (71a), (71b), (73a), and (73b) are the compact form of the fundamental equations for frequency-domain multiple scattering of a monochromatic electromagnetic plane wave by a collection of spherical particles at known positions [25,52]. They are the analog of Eqs. (32) and (33) for point-particle scattering and Eqs. (55) and (58) for scattering of scalar waves by spheres, and may be easily generalized to shaped-beam incidence. When Eqs. (73a) and (73b) are iterated and substituted into Eqs. (71a) and (71b), one obtains the expanded form of the total scattered fields [11].

Now consider the time-domain situation with a Gaussian electromagnetic pulse analogous to Eq. (19) incident on the collection of particles. The vector spherical wave function translation coefficients $A_{m_i, n_i; m_j, n_j}^H(\mathbf{r}_{ji})$ and $B_{m_i, n_i; m_j, n_j}^H(\mathbf{r}_{ji})$ are again sums over q , where $|m_j - n_j| \leq q \leq n_j + n_i$, of a product of a number of factors including $h_q^{(1)}(kr_{ji})$. For $kr_{ji} \gg q + 1/2$, this outgoing spherical Hankel function has the far-zone limit of Eq. (53a), producing exactly the same dominant rapidly-varying k -dependent phase factors as encountered in the geometrically simpler examples of Sections 4 and 5. The expanded form of the scattered fields is multiplied by the spectrum function of the incident pulse (20) and by $\exp(-ikct)$ corresponding to the linear dispersion relation for electromagnetic waves in the external medium. The result is then inverse Fourier transformed with respect to k , and the same sequence of time-delayed multiply-scattered pulses as in Sections 4 and 5 is generated. In addition, the rapidly-varying k -dependent phase factors contained in the Debye series decomposition of the partial wave scattering amplitudes $a_{n_j}^j$ and $b_{n_j}^j$ will produce fine-structure observed for each of the pulses that will eventually lead to gradual broadening. Thus the pulse sequences occur for electromagnetic scattering in exactly the same way they did for scalar wave scattering, and with the exception of the Debye series fine-structure broadening, for scattering by point-particles as well.

7. Scattering of a scalar wave by a collection of particles of finite size and arbitrary shape and composition

The partial wave sums in the examples of Sections 5 and 6 took advantage of the spherical symmetry of all the scattering particles in order to obtain the sets of coupled algebraic equations of the shape coefficients of Eqs. (58), (73a), and (73b) that were iterated to produce the multiple-particle paths in the frequency-domain. If the scattering particles have more complicated shapes, the symmetry is lost and another approach must be taken to obtain the appropriate coupled algebraic equations. In this example we use the T-matrix formalism (see for example Secs. 19.3 and 19.14 of [53] for details concerning the T-matrix in quantum mechanical scattering), and for simplicity we examine scattering of a scalar wave obeying a time-dependent Schrödinger-like equation as in Eq. (75) given below. The advantages of this alternative approach are that (i) it is applicable to particles of all shapes, including

spheres, and (ii) one does not need to transform various equations back and forth between different coordinate systems using sets of complicated translation coefficients. The drawback is that without taking advantage of spherical symmetry as was done in Sections 5 and 6, it will be much more difficult to obtain a suitable set of coupled algebraic equations for iteration. As was the case in the examples of Sections 4–6, we first describe scattering by a single particle which we call j , after which we describe multiple scattering by N particles with $1 \leq j \leq N$.

Particle j has arbitrary shape (which may or may not be a sphere), volume v_j , and arbitrary inhomogeneous internal composition which is represented by the well potential $V^j(\mathbf{r}'_{j0})$, where \mathbf{r}'_{j0} is the position of an arbitrary point inside particle j with respect to the origin. The geometric center of j is located at the known position \mathbf{r}_{j0} . Assuming monochromatic plane wave incidence, the total wave is again assumed to have the form

$$\psi_{total}(\mathbf{r}_{p0}, t) = \psi_{total}(\mathbf{r}_{p0}) \exp(-i\omega t). \quad (74)$$

The time dependence will again temporarily be left implicit. Upon inserting Eq. (74) into the time-dependent wave equation, the resulting time-independent Schrödinger-like equation is

$$\nabla^2 \psi(\mathbf{r}_{p0}) + CV(\mathbf{r}_{p0})\psi(\mathbf{r}_{p0}) = k^2 \psi(\mathbf{r}_{p0}), \quad (75)$$

where C is a constant of proportionality whose value depends on the type of scalar wave considered. Eq. (75) can be Fourier transformed, formally solved, and then inverse Fourier transformed to give an integral equation, known as the Lippmann–Schwinger equation (see Sec. 11.4.1 of [37]), that is equivalent to the original differential equation,

$$\psi_{total}(\mathbf{r}_{p0}) = \psi_0 \exp(i\mathbf{k}_{inc} \cdot \mathbf{r}_{p0}) - \frac{C}{4\pi v_j} \int d^3 r'_{j0} \frac{\exp(ikr'_{pj})}{r'_{pj}} V^j(\mathbf{r}'_{j0}) \psi_{total}(\mathbf{r}'_{j0}), \quad (76)$$

where \mathbf{r}'_{pj} is the position of the point p with respect to an arbitrary location inside j . The advantage of the integral equation formalism over the original differential equation formalism is that the boundary conditions are incorporated into the equation itself rather than having to be imposed separately after the most general solution of the differential equation has been obtained. The disadvantage is that one has to now deal with an integral equation, which is usually less familiar than is the original differential equation.

Our goal is to rewrite Eq. (76) in a form that hides the fact that it is an integral equation for as long as possible, and then isolates the integral equation nature into a hopefully easily controlled or easily calculable quantity. Decomposing the total wave into the sum of an incident plane wave and the wave scattered by particle j ,

$$\psi_{total}(\mathbf{r}_{p0}) = \psi_0 \exp(i\mathbf{k}_{inc} \cdot \mathbf{r}_{p0}) + \psi_{scatt}^j(\mathbf{r}_{p0}), \quad (77)$$

the scattered wave can be written as

$$\psi_{scatt}^j(\mathbf{r}_{p0}) = -\frac{C}{4\pi v_j} \int d^3 r'_{j0} \int_{v_j} d^3 r''_{j0} \frac{\exp(ikr'_{pj})}{r'_{pj}} \times T^j(\mathbf{r}'_{j0}, \mathbf{r}''_{j0}) \psi_0 \exp(i\mathbf{k}_{inc} \cdot \mathbf{r}''_{j0}) \quad (78)$$

where \mathbf{r}'_{j0} and \mathbf{r}''_{j0} are two different arbitrary locations inside j with respect to the origin, and $T^j(\mathbf{r}'_{j0}, \mathbf{r}''_{j0})$ is the single-particle transition operator or T-matrix for scattering by particle j . The T-matrix is the solution of the following equation:

$$T^j(\mathbf{r}'_{j0}, \mathbf{r}''_{j0}) = V^j(\mathbf{r}'_{j0}) \delta(\mathbf{r}'_{j0} - \mathbf{r}''_{j0}) - \frac{C}{4\pi} V^j(\mathbf{r}'_{j0}) \int_{v_j} d^3 r''_{j0} \frac{\exp(ik|\mathbf{r}'_{j0} - \mathbf{r}''_{j0}|)}{|\mathbf{r}'_{j0} - \mathbf{r}''_{j0}|} T^j(\mathbf{r}''_{j0}, \mathbf{r}''_{j0}), \quad (79)$$

where $\delta(\mathbf{r})$ is the three-dimensional delta function. Although Eq. (78) now has the form of a double volume integral to be evaluated, the fact that the original Eq. (76) is an integral equation is reflected in the fact that Eq. (79) is an integral equation in T^j . Physically Eq. (79), when iterated with $V^j C / 4\pi$ being small enough so that the iteration series converges, describes coherent multiple scattering inside particle j , beginning at the point \mathbf{r}''_{j0} and ending at \mathbf{r}'_{j0} . The single-particle T-matrix is said to be nonlocal or non-diagonal in coordinate space (see p. 520 of [23]) because the scattering interaction it describes does not occur at a single point inside j , but depends on both \mathbf{r}'_{j0} and \mathbf{r}''_{j0} . The first term in Eq. (79), when integrated, describes single-scattering by the well potential V^j at \mathbf{r}'_{j0} which is local, or diagonal in coordinate space, since $\mathbf{r}'_{j0} = \mathbf{r}''_{j0}$. The nonlocality is contained in the second term, which is the interior multiple-scattering series.

For the far-zone point p with respect to the origin such that $r_{p0} \gg r'_{j0}$ and $2r_{p0} \gg r''_{j0}$, one has

$$\mathbf{k}'_{pj} \approx \mathbf{k}r_{p0} - \mathbf{k}u_{scatt} \cdot \mathbf{r}'_{j0}. \quad (80)$$

Further, expressing an arbitrary position inside j with respect to the origin in terms of \mathbf{r}_{j0} and ρ'_j , the arbitrary position inside j with respect to the geometric center of j , we have

$$\mathbf{r}'_{j0} = \mathbf{r}_{j0} + \rho'_j, \quad (81a)$$

$$\mathbf{r}''_{j0} = \mathbf{r}_{j0} + \rho''_j. \quad (81b)$$

The far-zone limit of Eq. (78) then becomes

$$\psi_{scatt}^j(\mathbf{r}_{p0}) \rightarrow \frac{C}{4\pi} \frac{\exp(ikr_{p0})}{r_{p0}} \exp[i(\mathbf{k}_{inc} - \mathbf{k}_{scatt}) \cdot \mathbf{r}_{j0}] \psi_0 \times \int_{v_j} d^3 \rho'_j \int_{v_j} d^3 \rho''_j \exp(-i\mathbf{k}_{scatt} \cdot \rho'_j) \times T^j(\mathbf{r}'_{j0}, \mathbf{r}''_{j0}) \exp(i\mathbf{k}_{inc} \cdot \rho''_j). \quad (82)$$

Since only \mathbf{k}_{scatt} and \mathbf{k}_{inc} remain after the two integrations in the second term of Eq. (82) are performed over the volume of the particle, we can define

$$f^j(\mathbf{k}_{scatt}, \mathbf{k}_{inc}, \Omega^j) \equiv \frac{C}{4\pi} \int_{v_j} d^3 \rho'_j \int_{v_j} d^3 \rho''_j \exp(-i\mathbf{k}_{scatt} \cdot \rho'_j) \times T^j(\mathbf{r}'_{j0}, \mathbf{r}''_{j0}) \exp(i\mathbf{k}_{inc} \cdot \rho''_j), \quad (83)$$

where Ω^j denotes the orientation of particle j with respect to the \mathbf{k}_{inc} direction. As a result, the far-zone limit is then

$$\psi_{scatt}^j(\mathbf{r}_{p0}) \rightarrow \frac{\exp(ikr_{p0})}{r_{p0}} f^j(\mathbf{k}_{scatt}, \mathbf{k}_{inc}, \Omega^j) \times \exp[i(\mathbf{k}_{inc} - \mathbf{k}_{scatt}) \cdot \mathbf{r}_{j0}] \psi_0. \quad (84)$$

The form of Eq. (84) suggests that Eq. (83) is the far-zone single-particle scattering amplitude as a function of the scattering angles θ_{p0} and φ_{p0} with respect to the origin's coordinate system. Theoretically, f^j is obtained by first using the explicit form of the T-matrix for the specific well potential of interest, and then performing all the integrals contained in the internal multiple-scattering series. This is a daunting job if the particle has an irregular shape or is inhomogeneous. Since the directions of \mathbf{k}_{inc} and \mathbf{k}_{scatt} are fixed in the origin's coordinate system, the scattering amplitude at the fixed far-zone detector will change as the particle's orientation Ω^j changes if particle j has an irregular shape. If the particle is spherical, then the scattering amplitude will be independent of Ω^j , but it will still be nonlocal. This is the price to be paid for no longer having enough symmetry to be able to use the partial wave approach as in the examples of Sections 5 and 6. As a result, the entirety of the complicated nature of the scattering pattern as a function of orientation is contained in the complex function f^j . Part of this complicated nature can be accessed experimentally since the measured scattered intensity for a given particle orientation is proportional to $|f^j|^2$. This measurement determines the amplitude of f^j , but leaves its phase undetermined.

For scattering of an incident monochromatic plane wave by N particles, the Lippmann–Schwinger equation now becomes

$$\psi_{total}(\mathbf{r}_{p0}) = \psi_0 \exp(i\mathbf{k}_{inc} \cdot \mathbf{r}_{p0}) - \frac{C}{4\pi} \sum_{j=1}^N \int_{V_j} d^3 r'_{j0} \frac{\exp(ikr'_{pj})}{r'_{pj}} V^j(\mathbf{r}'_{j0}) \psi_{total}(\mathbf{r}'_{j0}), \quad (85)$$

assuming that the general scattering object of Eq. (76) has been decomposed into the N distinct (i.e. non-overlapping) scattering particles. It has been shown [17] that this integral equation is equivalent to

$$\psi_{total}(\mathbf{r}_{p0}) = \psi_0 \exp(i\mathbf{k}_{inc} \cdot \mathbf{r}_{p0}) - \frac{C}{4\pi} \sum_{j=1}^N \int_{V_j} d^3 r'_{j0} \int_{V_j} d^3 r''_{j0} \frac{\exp(ikr'_{pj})}{r'_{pj}} \times T^j(\mathbf{r}'_{j0}, \mathbf{r}''_{j0}) \psi_{inc}^j(\mathbf{r}''_{j0}), \quad (86)$$

where ψ_{inc}^j is the wave incident on particle j evaluated at the arbitrary position \mathbf{r}''_{j0} inside j , and T^j is the single-particle T-matrix of Eq. (79). Written in this way, Eq. (86) looks like a double volume integral to be evaluated, rather than explicitly taking the form of an integral equation. The integral equation nature is hidden both in T^j , which was discussed above, and in ψ_{inc}^j . Specifically, $\psi_{inc}^j(\mathbf{r}''_{j0})$ is the sum of the incident plane wave and the wave scattered by all the other particles,

$$\psi_{inc}^j(\mathbf{r}''_{j0}) = \psi_0 \exp(i\mathbf{k}_{inc} \cdot \mathbf{r}''_{j0}) + \sum_{i=1}^j \psi_{scatt}^i(\mathbf{r}''_{j0}) \quad (87)$$

where $\psi_{scatt}^i(\mathbf{r}''_{j0})$ is the scattered wave created at particle i and evaluated at the arbitrary position \mathbf{r}''_{j0} inside particle j . This scattered wave has been shown to have the form [17]

$$\psi_{scatt}^i(\mathbf{r}''_{j0}) = -\frac{C}{4\pi} \int_{V_i} d^3 r'_{i0} \int_{V_i} d^3 r''_{i0} \frac{\exp(ik|\mathbf{r}''_{j0} - \mathbf{r}'_{i0}|)}{|\mathbf{r}''_{j0} - \mathbf{r}'_{i0}|}$$

$$\times T^i(\mathbf{r}'_{i0}, \mathbf{r}''_{i0}) \psi_{inc}^i(\mathbf{r}''_{i0}). \quad (88)$$

Eqs. (86)–(88) are known as the Foldy–Lax equations [8,16], and are considered as the fundamental equations in compact form for the multiple scattering of waves by particles at known positions and having arbitrary properties. If Eq. (88) is substituted into Eq. (87) one obtains a set of coupled integral equations for the $\psi_{inc}^j(\mathbf{r}''_{j0})$, the solution of which can then be inserted into Eq. (86). If on the other hand Eq. (87) is substituted into Eq. (88), one obtains a set of coupled integral equations for the $\psi_{scatt}^i(\mathbf{r}''_{j0})$.

Taking this second point of view and using Eq. (81b) along with

$$\mathbf{r}'_{i0} = \mathbf{r}_{i0} + \rho'_i, \quad (89a)$$

$$\mathbf{r}''_{i0} = \mathbf{r}_{i0} + \rho''_i, \quad (89b)$$

the set of coupled integral equations for $\psi_{scatt}^i(\mathbf{r}''_{j0})$ becomes

$$\begin{aligned} \psi_{scatt}^i(\mathbf{r}''_{j0}) = & -\frac{C}{4\pi r_{ji}} \exp[i\mathbf{k}_{ji} \cdot (\mathbf{r}_{j0} - \mathbf{r}_{i0})] \\ & \times \exp(i\mathbf{k}_{inc} \cdot \mathbf{r}_{i0}) \int_{V_i} d^3 \rho'_i \int_{V_i} d^3 \rho''_i \\ & \times \exp[-i\mathbf{k}_{ji} \cdot (\rho'_i - \rho''_i)] T^i(\mathbf{r}'_{i0}, \mathbf{r}''_{i0}) \exp(i\mathbf{k}_{inc} \cdot \rho''_i) \psi_0 \\ & - \frac{C}{4\pi r_{ji}} \sum_{m=1}^N \exp[i\mathbf{k}_{ji} \cdot (\mathbf{r}_{j0} - \mathbf{r}_{i0})] \int_{V_i} d^3 \rho'_i \int_{V_i} d^3 \rho''_i \\ & \times \exp[-i\mathbf{k}_{ji} \cdot (\rho'_i - \rho''_i)] T^i(\mathbf{r}'_{i0}, \mathbf{r}''_{i0}) \psi_{scatt}^m(\mathbf{r}''_{i0}). \quad (90) \end{aligned}$$

Our goal is to convert these coupled integral equations into a set of coupled algebraic equations, which can be numerically solved much more easily. This is accomplished in the following way. Let new functions $\xi_{scatt}^i(\mathbf{r}''_{j0})$ and $\xi_{scatt}^m(\mathbf{r}''_{i0})$ be defined by

$$\psi_{scatt}^i(\mathbf{r}''_{j0}) \equiv \exp[i\mathbf{k}_{ji} \cdot (\mathbf{r}_{ji} + \rho''_i)] \xi_{scatt}^i(\mathbf{r}''_{j0}), \quad (91a)$$

$$\psi_{scatt}^m(\mathbf{r}''_{i0}) \equiv \exp[i\mathbf{k}_{im} \cdot (\mathbf{r}_{im} + \rho'_i)] \xi_{scatt}^m(\mathbf{r}''_{i0}). \quad (91b)$$

Substituting Eqs. (91a) and (91b) into Eq. (90) one obtains

$$\begin{aligned} \xi_{scatt}^i(\mathbf{r}''_{j0}) = & -\frac{C}{4\pi r_{ji}} \exp(i\mathbf{k}_{inc} \cdot \mathbf{r}_{i0}) \int_{V_i} d^3 \rho'_i \int_{V_i} d^3 \rho''_i \\ & \times \exp(-i\mathbf{k}_{ji} \cdot \rho'_i) T^i(\mathbf{r}'_{i0}, \mathbf{r}''_{i0}) \exp(i\mathbf{k}_{inc} \cdot \rho''_i) \\ & - \frac{C}{4\pi r_{ji}} \sum_{m=1}^N \exp[i\mathbf{k}_{im} \cdot (\mathbf{r}_{i0} - \mathbf{r}_{m0})] \int_{V_i} d^3 \rho'_i \\ & \times \int_{V_i} d^3 \rho''_i \exp(-i\mathbf{k}_{ji} \cdot \rho'_i) T^i(\mathbf{r}'_{i0}, \mathbf{r}''_{i0}) \\ & \times \exp(i\mathbf{k}_{im} \cdot \rho'_i) \xi_{scatt}^m(\mathbf{r}''_{i0}). \quad (92) \end{aligned}$$

One notices that the right hand side of Eq. (92) does not depend on ρ''_j . Thus $\xi_{scatt}^i(\mathbf{r}''_{j0})$ must only be a function of \mathbf{r}_{j0} and not of ρ''_j (see Eq. (81b)). Similarly, if this equation were instead written for $\xi_{scatt}^m(\mathbf{r}''_{i0})$, again the right hand side of the equation would only be a function of \mathbf{r}_{i0} and would not depend on ρ''_i (see Eq. (89b)). As a result, $\xi_{scatt}^m(\mathbf{r}_{i0})$ can be moved outside the integral over ρ''_i in the second term of Eq. (92). Then using the definition of the far-zone single-particle scattering amplitude of Eq. (83) in order to hide the last remnant of the integral equation nature of the situation, Eq. (92) simplifies to

$$\begin{aligned} \xi_{scatt}^i(\mathbf{r}_{j0}) &= \frac{1}{r_{ji}} \exp(i\mathbf{k}_{inc} \cdot \mathbf{r}_{i0}) f^i(\mathbf{k}_{ji}, \mathbf{k}_{inc}, \Omega^i) \psi_0 \\ &+ \frac{1}{r_{ji}} \sum_{m=1}^N \exp[i\mathbf{k}_{im} \cdot (\mathbf{r}_{i0} - \mathbf{r}_{m0})] \\ &\times f^j(\mathbf{k}_{ji}, \mathbf{k}_{im}, \Omega^i) \xi_{scatt}^m(\mathbf{r}_{i0}). \end{aligned} \quad (93)$$

This is the desired set of coupled algebraic equations, assuming all the particles are in the far-zone of each other and the single-particle scattering amplitudes f^j are known [21]. The only remnant of the original integral equations lies in the relation of f^i to the integral equation (79) for the single-particle T-matrix. Once these coupled algebraic equations are solved by iteration and inserted into Eqs. (91a) and (91b), then into Eq. (87), and finally into Eq. (86), one obtains the expanded form for the total wave at any point in space with respect to the origin. For scattering by a collection of homogeneous spheres, the single-particle scattering amplitude $f^j(\mathbf{k}_{scatt}, \mathbf{k}_{inc})$ may be explicitly written as a sum over partial waves, so that the coupled algebraic equations of Eq. (93) reduce to coupled partial wave beam shape coefficients as in Eq. (58) of Section 5.

If one is interested in far-zone scattering, Eq. (86) and (87) substantially simplify. Using Eq. (83) and

$$\mathbf{k}\mathbf{r}'_{pj} \approx \mathbf{k}\mathbf{r}_{p0} - \mathbf{k}\mathbf{u}_{p0} \cdot \mathbf{r}'_{j0} = \mathbf{k}\mathbf{r}_{p0} - \mathbf{k}\mathbf{u}_{p0} \cdot \mathbf{r}_{j0} - \mathbf{k}\mathbf{u}_{p0} \cdot \rho'_j, \quad (94)$$

Eq. (86) becomes

$$\begin{aligned} \psi_{total}(\mathbf{r}_{p0}) &= \psi_0 \exp(i\mathbf{k}_{inc} \cdot \mathbf{r}_{p0}) \\ &+ \frac{\exp(i\mathbf{k}\mathbf{r}_{p0})}{r_{p0}} \sum_{j=1}^N \exp[i(\mathbf{k}_{inc} - \mathbf{k}_{scatt}) \cdot \mathbf{r}_{j0}] \\ &\times f^j(\mathbf{k}_{scatt}, \mathbf{k}_{inc}, \Omega^j) \psi_0 \\ &+ \frac{\exp(i\mathbf{k}\mathbf{r}_{p0})}{r_{p0}} \sum_{j=1}^N \exp[i(\mathbf{k}_{inc} - \mathbf{k}_{scatt}) \cdot \mathbf{r}_{j0}] \\ &\times \sum_{i=1}^N \exp(-i\mathbf{k}_{ji} \cdot \mathbf{r}_{i0}) f^j(\mathbf{k}_{scatt}, \mathbf{k}_{ji}, \Omega^j) \xi_{scatt}^i(\mathbf{r}_{j0}). \end{aligned} \quad (95)$$

As was the case in the examples of Sections 4–6, all the dominant k-dependent phases have now been explicitly separated out in Eqs. (93) and (95). These phases separated out straightforwardly in the examples of Sections 3 and 4. But some of them were implicit in the translation coefficients in the examples of Sections 5 and 6. Here some of them rely on the introduction of the subsidiary functions of Eqs. (91a) and (91b). Although the phases may always be separated out, the details of the separation are seen to depend on the differing mathematical approaches taken in the different examples. In order to obtain the time-domain equations, the iterated version of Eqs. (93) and (95) are multiplied by the spectrum function of an incident pulse of Eq. (20) and $\exp(-ikct)$ corresponding to a linear dispersion relation in the external medium. The result is then inverse Fourier transformed with respect to k, and one obtains exactly the same temporal sequence of pulses that occurred for the earlier examples.

If one were interested in scattering of an electromagnetic wave by a collection of particles of finite size and arbitrary shape and composition, the situation is most conveniently described using the dyadic formalism. The derivation of the

scattering formulas is treated completely in Chapter 6 of [6], and no further elaboration on the method is required here. In time-domain scattering with an incident Gaussian pulse for this example, the same k-dependent phases can be explicitly separated out and the same time-dependent pulse sequences will again occur.

8. Conclusions

In this tutorial, we examined the multiple scattering equations for a scalar (or electromagnetic) plane wave or plane wave pulse incident on a collection of particles at known positions. In one example the particles were all infinitesimally small. In another they were all spheres, and in yet another they all had arbitrary shape and internal composition. As a prelude to these calculations we also considered the one-dimensional example of a plane wave or plane wave pulse normally incident on a block of nonabsorptive material having two flat parallel faces. In each of these examples the multiple scattering equations were derived using different mathematical approaches which were tailored to the differing symmetry character of the situations. There are certain features of multiple scattering that differ from example to example, depending on the specific nature of the incident beam and scattering particles. The most obvious of these is the need to keep track of the polarization state of multiply-scattered electromagnetic waves, which is not an issue for scalar waves. Similarly, the sharp forward peaking of diffractive scattering by a single particle whose radius is much larger than the wavelength results in forward peaking of the light multiply-scattered by a collection of large particles. On the other hand, isotropic scattering by a single point-particle results in nearly isotropic multiple scattering by a collection of point-particles.

From a comparison of the multiple scattering equations for the different examples we considered, we made a number of general statements concerning frequency-domain multiple scattering. First, even in the context of single scattering, since the total wave is the exact solution of the appropriate wave equation boundary value problem that has been posed, it has a definite physical existence and has an undeniable degree of primacy over the incident beam and scattered wave of which it is composed. However, since the incident beam and scattered wave have attributes such as direction of travel or polarization state that differ from each other at most scattering angles, the difference can be exploited to filter out one of the components so that all or a portion of the energy content of the remaining component can be measured. In this way the incident beam and scattered wave, individually, are endowed with a level of physical significance that transcends the infinite number of other possible purely mathematical decompositions of the total wave.

Second, frequency-domain multiple scattering is a steady state situation resulting from the infinite temporal duration of the incident wave. Thus all the scatterings and rescatterings that can occur are always occurring. There is no time dependence for one scattering to occur first, the next scattering to occur at a later time, the third scattering to occur at yet a later time, etc. In addition, although the multiple scattering

equations when written in expanded form can be interpreted as a complete collection of multi-particle paths that is suggestive of multiple scattering, the presence of the multi-particle paths is obscured when the equations are written in their compact form. As a result of the lack of temporal information in the frequency-domain equations and the ability to transform away the multi-particle path interpretation by using another form of the equations, we conclude that frequency-domain multiple scattering is purely a mathematical abstraction.

On the other hand, there are certain features of time-domain multiple scattering which occur in the same way, or persist, no matter what type of beam or particle is considered. When the collection of particles is tenuous rather than close-packed, and the scattering interaction is sufficiently weak so that the iteration series converges, scattering of a temporally-short pulse results in a temporal succession of distinct individual scattered pulses in a one-to-one correspondence with the different multi-particle paths in the frequency-domain. This temporal succession was found to persist for all the different examples we considered in this tutorial, and the individual time-delayed pulses in the sequence are readily measurable. Mathematically, the expanded solution to the multiple scattering equations in the time domain under these conditions would appear to be the only form of the solution there is, once the inverse Fourier transform involved has been evaluated either analytically or numerically. Since the pulse train cannot be transformed away by writing the solution to the scattering equations in a different form, when a localized pulse is incident on the collection of particles, time-domain multiple scattering becomes a definite physical phenomenon.

Acknowledgment

We thank two anonymous reviewers for their constructive and helpful comments. MIM appreciates support from the NASA Remote Sensing Theory Program managed by Lucia Tsoussi and the NASA Radiation Sciences Program managed by Hal Maring.

References

- [1] Martin PA. Multiple scattering: interaction of time-harmonic waves with N obstacles. Cambridge, UK: Cambridge University Press; 2006.
- [2] Mishchenko MI. Gustav Mie and the fundamental concept of electromagnetic scattering by particles: a perspective. *J Quant Spectrosc Radiat Transf* 2009;110:1210–22.
- [3] Mishchenko MI, Tishkovets VP, Travis LD, Cairns B, Dlugach JM, Liu L, et al. Electromagnetic scattering by a morphologically complex object: fundamental concepts and common misconceptions. *J Quant Spectrosc Radiat Transf* 2011;112:671–92.
- [4] Mishchenko MI. Directional radiometry and radiative transfer: a new paradigm. *J Quant Spectrosc Radiat Transf* 2011;112:2079–94.
- [5] Mishchenko MI. Directional radiometry and radiative transfer: the convoluted path from centuries-old phenomenology to physical optics. *J Quant Spectrosc Radiat Transf* 2014;146:4–33.
- [6] Mishchenko MI. Electromagnetic scattering by particles and particle groups: an introduction. Cambridge, UK: Cambridge University Press; 2014.
- [7] Twersky V. On propagation in random media of discrete scatterers. In: Bellman R, editor. Stochastic processes in mathematical physics and engineering. Providence, RI: American Mathematical Society; 1964. p. 84–116.
- [8] Lax M. Multiple scattering of waves. *Rev Mod Phys* 1951;23:287–310.
- [9] Twersky V. Multiple scattering of radiation by an arbitrary configuration of parallel cylinders. *J Opt Soc Am* 1952;24:42–6.
- [10] Twersky V. Multiple scattering by arbitrary configurations in three dimensions. *J Math Phys* 1962;3:83–91.
- [11] Fuller KA, Kattawar GW. Consumate solution to the problem of classical electromagnetic scattering by an ensemble of spheres. I: linear chains. *Opt Lett* 1988;13:90–2.
- [12] Goldberger M, Watson KM. Collision theory. New York: Wiley; 1964.
- [13] van de Hulst H. Light scattering by small particles. New York: Dover; 1981.
- [14] Brillouin L. The scattering cross section of spheres for electromagnetic waves. *J Appl Phys* 1949;20:1110–25.
- [15] Nussenzveig HM. High-frequency scattering by an impenetrable sphere. *Ann Phys (NY)* 1965;34:23–95.
- [16] Foldy LL. The multiple scattering of waves. *Phys Rev* 1945;67:107–19.
- [17] Watson KM. Multiple scattering and the many-body problem – applications to photomeson production in complex nuclei. *Phys Rev* 1953;89:575–87.
- [18] MacKintosh FC, John S. Diffusing-wave spectroscopy and multiple scattering of light in correlated random media. *Phys Rev B* 1989;40:2383–406.
- [19] Weitz DA, Pine DJ. Diffusing-wave spectroscopy. In: Brown W, editor. Dynamic light scattering, the method and some applications. Oxford, UK: Clarendon Press; 1993. p. 652–720.
- [20] Ishimaru A. Wave propagation and scattering in random media. New York: Academic Press; 1978.
- [21] Mishchenko MI. Vector radiative transfer equation for arbitrarily shaped and arbitrarily oriented particles: a microphysical derivation from statistical electromagnetics. *Appl Opt* 2002;41:7114–34.
- [22] Watson KM. Multiple scattering by quantum-mechanical systems. *Phys Rev* 1957;105:1388–98.
- [23] Merzbacher E. Quantum mechanics. New York: Wiley; 1970.
- [24] Fuller KA. Optical resonances and two-sphere systems. *Appl Opt* 1991;30:4716–31.
- [25] Fuller KA, Mackowski DW. Electromagnetic scattering by compounded spherical particles. In: Mishchenko MI, Hovenier JW, Travis LD, editors. Light scattering by nonspherical particles. San Diego, CA: Academic Press; 2000. p. 225–72.
- [26] Nussenzveig HM. Diffraction effects in semiclassical scattering. Cambridge, UK: Cambridge University Press; 1992.
- [27] Hale GM, Querry MR. Optical constants of water in the 200-nm to 200- μ m wavelength region. *Appl Opt* 1973;12:555–63.
- [28] Jenkins FA, White HE. Fundamentals of optics. New York: McGraw-Hill; 1950.
- [29] Griffiths DJ. Introduction to electrodynamics. Upper Saddle River, NJ: Prentice Hall; 1991.
- [30] Goldberg A, Schey HM, Schwartz JL. Computer-generated motion pictures of one-dimensional quantum-mechanical transmission and reflection phenomena. *Am J Phys* 1967;35:177–86.
- [31] Hecht E. Optics. Reading, MA: Addison-Wesley; 1987.
- [32] Nussenzveig HM. High-frequency scattering by a transparent sphere. I. Direct reflection and transmission. *J Math Phys* 1969;10:82–124.
- [33] Nussenzveig HM. High-frequency scattering by a transparent sphere. II. Theory of the rainbow and the glory. *J Math Phys* 1969;10:125–76.
- [34] Lock JA. Cooperative effects among partial waves in Mie scattering. *J Opt Soc Am A* 1988;5:2032–44.
- [35] Lock JA, Laven P. Understanding light scattering by a coated sphere. Part 1: theoretical considerations. *J Opt Soc Am A* 2012;29:1489–97.
- [36] Jackson JD. Classical electrodynamics. New York: Wiley; 1962.
- [37] Griffiths DJ. Introduction to quantum mechanics. Upper Saddle River, NJ: Pearson-Prentice Hall; 2005.
- [38] Laven P. Time domain analysis of scattering by a water droplet. *Appl Opt* 2011;50:F29–38.
- [39] Mattuck RD. A guide to Feynman diagrams in the many-body problem. New York: Dover; 1976.
- [40] Friedman B, Russek J. Addition theorems for spherical waves. *Quart Appl Math* 1954;12:13–23.
- [41] Stein S. Addition theorems for spherical wave functions. *Quart Appl Math* 1961;19:15–24.
- [42] Cruzan OR. Translational addition theorems for spherical vector wave functions. *Quart Appl Math* 1962;20:33–40.
- [43] Tam WG, Coriveau R. Scattering of electromagnetic beams by spherical objects. *J Opt Soc Am* 1978;68:763–7.
- [44] Mackowski DW. Analysis of radiative scattering for multiple sphere configurations. *Proc R Soc Lond A* 1991;433:599–614.
- [45] Xu Y-L. Electromagnetic scattering by an aggregate of spheres. *Appl Opt* 1995;34:4573–88 Errata: 1998;37:6494, 2001;40:5508.

- [46] Xu Y-L. Electromagnetic scattering by an aggregate of spheres; far field. *Appl Opt* 1997;36:9496–508.
- [47] Abramowitz M, Stegun I. *Handbook of mathematical functions*. Washington DC: National Bureau of Standards; 1964.
- [48] Lock JA. Electric field autocorrelation functions for beginning multiple Rayleigh scattering. *Appl Opt* 2001;40:4187–203.
- [49] Barton JP, Ma W, Schaub SA, Alexander DR. Electromagnetic field for a beam incident on two adjacent spherical particles. *Appl Opt* 1991;30:4707–15.
- [50] Tsang L, Kong JA, Shin RT. *Theory of microwave remote sensing*. New York: Wiley; 1985.
- [51] Mishchenko MI, Travis LD, Lacis AA. *Scattering, absorption and emission of light by small particles*. Cambridge, UK: Cambridge University Press; 2002.
- [52] Mackowski D. The extension of Mie theory to multiple spheres. In: Hergert T, Wriedt T, editors. *The Mie theory*. Berlin: Springer; 2012. p. 223–56.
- [53] Messiah A. *Quantum mechanics*, vol. 2. New York: Wiley; 1966.